

FERMILAB-Proposal-0489

Fermilab Proposal No. 489  
Scientific Spokesman: F. A. Nezrick  
Fermi National Accelerator Laboratory  
P. O. Box 500  
Batavia, Illinois 60510  
FTS/Commercial (312) 840-3201

PROPOSAL TO STUDY NEUTRINO INTERACTIONS IN HYDROGEN AND NUCLEI  
WITH AN INTERNAL TARGET AND CONVERTER SYSTEM IN THE  
15-FT. BUBBLE CHAMBER

J. P. Berge, F. A. DiBianca, R. Hanft, F. A. Nezrick,  
W. G. Scott and W. Smart

Fermi National Accelerator Laboratory,  
Batavia, Illinois 60510

April, 1976

104pgs.

## ABSTRACT

We propose a study of broad-band neutrino interactions on free protons and simultaneously on nuclei with 90% gamma conversion, 95% electron and muon identification by using an Internal Target and Converter (ITC) system in the 15-Ft. chamber. We request an exposure of 300,000 pictures with  $1.3 \times 10^{13}$  protons per pulse of energy 400 GeV. Based on measured yields from E-45 we expect 100,000 neutrino events in this exposure. The physics program includes studies of  $\mu^-e^+$  and  $\mu^-\mu^+$  production; searches for charmed particles,  $\psi$ 's, heavy leptons, intermediate vector bosons and other new particles; comparisons of  $\nu p$  and  $\nu n$  interactions including precision measurements of  $\sigma(n)/\sigma(p)$  for both charged and neutral currents; charged and neutral current deep inelastic scattering; detailed studies of exclusive channels including  $\pi^0$ 's,  $V^0$ 's and kinks in both charged and neutral current reactions; pure leptonic interactions; and charged and neutral particle multiplicity distributions in both charged and neutral current reactions.

## TABLE OF CONTENTS

- I. Introduction
- II. Description of the ITC System
  - A. Simultaneous Studies of Neutrino Interactions on Free Nucleons and Heavy Nuclei
  - B. High Efficiency  $\gamma$  Conversion
  - C. Momentum Resolution of Charged Hadrons
  - D. Corresponding Point Measurements
  - E. Identification of Charged Leptons
    - 1. Electrons
    - 2. Muons
  - F. Hydrogen Fiducial Volume
  - G.  $\nu$ -Nucleus Interactions
  - H. Additional Features of the ITC System
    - 1. Measurement of Backgrounds
    - 2. Visual Determination of  $x, y, z$  of Points on Tracks
    - 3. Independence of  $\bar{l}_\gamma$  and  $\bar{l}_{\text{hadrons}}$
- III. Physics
  - A. Study of Di-lepton Production
  - B. New Particle Searches
    - 1. Charmed Particle Production
    - 2. Diffractive  $\psi$  Production by Weak Neutral Current
    - 3. Heavy Lepton Production
    - 4. Intermediate Vector Boson Production
    - 5. Production of Other New Particles

(ii)

- C. Measurement of  $\sigma(n)/\sigma(p)$  for Charged and Neutral Currents
- D. Deep Inelastic Scattering
  - 1. Charged Current Reactions
  - 2. Neutral Current Reactions
- E. Exclusive Channels
  - 1. Resonance Production
    - a. Meson Resonances
    - b. Baryon Resonances
    - c. Double Resonance Production
  - 2. Strange Particle Production
    - a. Charged Currents
    - b. Neutral Currents
- F. Heavy Particle Production from Nuclei
- G. Pure Leptonic Interactions
- H. Charged and Neutral Particle Multiplicity Distributions

APPENDIX A. Details of ITC

APPENDIX B. Comparison of ITC, Downstream Plate Array, TST and H<sub>2</sub>-Ne Chambers

We propose to build an Internal Target and Converter (ITC) System for the 15-ft chamber. We request an exposure of 300 K photographs of broad-band neutrinos in the 15-ft chamber with a hydrogen fill and ITC to study  $\nu p$  and  $\nu$  nucleus interactions in both inclusive and exclusive channels.

### I. INTRODUCTION

Major goals of neutrino experiments which have not been achieved in a single experiment are:

- (1) large yields of events for physics analysis and also for background studies,
- (2) comparisons of neutrino (antineutrino) reactions on free protons (or quasi-free protons and neutrons in deuterium) as well as on nuclear targets in one experiment to measure relative cross sections on u and d-quarks in circumstances where flux uncertainties and many other systematic effects become irrelevant,
- (3) ability to separate to better than 95 percent and to analyze charged and neutral current events.
- (4) measurement of the incident neutrino energy to better than 5 percent for charged current reactions and to ~ 15 percent accuracy for neutral current reactions,
- (5) detection and measurement of neutral particles - particularly neutrons,  $\pi^0$ 's and single  $\gamma$ 's,
- (6) ability to perform constrained kinematic fits on a large fraction of the  $H_2$  events including final states containing a neutron,  $\pi^0$ 's and/or single  $\gamma$ 's.
- (7) ability to detect and study both  $V^0$  and kink-type

strange particles - i.e.,  $K^0$ ,  $\Lambda^0$ ,  $\bar{\Lambda}$ ,  $K^\pm$ ,  $\Sigma^\pm$ ,  
 $\Xi^-$ ,  $\Xi^0$ ,

- (8) ability to unscramble automatically (i.e., track match) high-multiplicity topologies as well as to discriminate between slow p, K,  $\pi$ ,  $\mu$ , e (measuring through any turning angle no matter how large) by measuring up to eleven (or more) corresponding points on each track in each view,
- (9) identification to better than 95 percent and measurement of outgoing electrons.
- (10) identification to better than 95 percent and measurement of outgoing muons (using EMI information).

We feel that all of the above goals can be achieved in a single ITC experiment.

## II. DESCRIPTION OF THE ITC SYSTEM

The ITC combines most of the best features of the hydrogen (or deuterium) bubble chamber, the heavy liquid bubble chamber and the track sensitive target while incorporating new features not found in any of these instruments.

Simple in concept and inexpensive as well, an ITC for the 15-ft. chamber consists of a series of (nine) thin steel\* plates, each 0.5 radiation lengths thick, and 30 cm. apart at the chamber mid-plane with areas encompassing the usual fiducial volume. Each plate is tilted to present minimum obscuration to two cameras (#5 and #6) while allowing partial visibility of each track segment in a third view (#1). The appearance of the chamber with the

\* stainless steel (non-magnetic)

proposed ITC configuration is shown in Fig. 1.

The general features of the ITC system are now discussed and further details are given in Appendix A.

A. Simultaneous Studies of Neutrino Interactions on Free Nucleons and Heavy Nuclei

The ITC system provides the capability to study simultaneously interactions on both free protons (or nearly free protons and neutrons in deuterium) and heavy nuclei. Since the two kinds of target are spatially separate, in contrast to H-Ne fills in which they are mixed, it is easy to identify the target in every event.

B. High Efficiency  $\gamma$  Conversion

The proposed ITC configuration provides 4.5 radiation lengths of metal plus 0.3 radiation lengths of hydrogen. The average  $\gamma$  conversion efficiency for events distributed uniformly throughout the fiducial volume is 90% for a 16 m<sup>3</sup> fiducial volume upstream of plate number 8. The  $\gamma$  conversion efficiency versus angle with respect to the  $\nu$  direction is shown in Fig. 2 for ITC, TST, a downstream plate array, pure Ne, 20% atomic Ne and pure H<sub>2</sub>. The ITC system fares very well in this comparison.

We now consider the resolution expected for  $\gamma$  momentum from ITC. Electrons, typically measurable for only ~ 30 cm in ITC, will have  $\Delta p/p$  of ~ 1% (~ 10%) for  $p \sim 1$  GeV/c (~ 10 GeV). Of course, further resolution can be obtained by measuring brem  $\gamma$ 's from primary electrons.

Since primary electrons see, on the average, 1/4 radiation lengths of steel before reaching the hydrogen it is important to consider electron straggling (via bremsstrahlung) in the

conversion plate. Figure 3 shows  $\phi(\alpha, t)$ , the probability that an electron retains a fraction  $\alpha$  of its incident energy after traversing  $t$  radiation lengths of steel. In both the Bethe-Heitler<sup>1</sup> and Mo-Tsai<sup>2</sup> approximation,  $\phi(\alpha, t)$  is independent of incident energy. We use the Mo-Tsai approximation which is more precise ( $< 2\%$ ). For  $t = 0.25$ ,  $\bar{\alpha} = 0.75$ , and  $\delta\alpha$  (r.m.s.) = 0.29. Thus,  $\delta p/p$  is 0.39 for one electron and  $\sim 0.31$  for a  $\gamma$ . This uncertainty can be reduced to about 0.10 by measuring brems  $\gamma$ 's. The corresponding  $\pi^0$  fractional momentum error is 0.17 (0.06 with brems  $\gamma$ 's) before fitting.

#### C. Momentum Resolution of Charged Hadrons

Since all tracks are detected and measured in hydrogen, the track reconstruction parameters are optimal. There are, however, two effects of the plates which must be considered: momentum resolution deterioration via multiple scattering and via track length reduction from strong interactions.

A typical (2 meter) track passes through 2.8 radiation lengths of converter and 0.2 radiation lengths of  $H_2$ . Then, as long as  $\beta \sim 1$ ,  $\Delta p/p$  from multiple scattering is  $< 2\%$ .

The mean free path for hadrons (2 GeV/c pions) is 2.4 m. in the proposed ITC configuration. The hadron interaction probability per plate is only 0.07. Thus, hadrons with momenta of several tens of GeV/c (which there are very few of) will typically have  $\Delta p/p < 2\%$ .

#### D. Corresponding Point Measurements

The points where tracks enter and leave each plate are corresponding points in space. Therefore each point can be reconstructed independently in space without performing track

orbit interpolations. Thus tracks can be measured through arbitrarily large turning angles. This is especially important in discriminating between slow pions and muons where the EMI is least effective.

Furthermore, the corresponding point reconstruction solves automatically all track match problems no matter how high the track multiplicity. In addition, computer time for geometrical reconstruction will decrease.

#### E. Identification of Charged Leptons

##### 1) Electrons

Electrons or arbitrary momenta will be identified after measurement with efficiency  $> 95\%$  from bremsstrahlung in the plates or via their characteristic spirals for low energies.

##### 2) Muons

Muons will be identified with efficiency  $> 95\%$  by a combination of the EMI, plate penetration and transverse momentum characteristics.<sup>3,7</sup> The plates will be most helpful in the angular region of  $60^\circ - 180^\circ$  where the EMI coverage is poor.

#### F. Hydrogen Fiducial Volume

The hydrogen fiducial volume in the proposed ITC system is  $16 \text{ m}^3$  which is only slightly less than for a bare chamber (i.e.,  $20 \text{ m}^3$ ). It is difficult to design a TST for the 15-ft chamber with a hydrogen fiducial volume of much more than  $4 \text{ m}^3$ .

G.  $\nu$ -Nucleus Interactions

The configuration of nine 0.9 cm stainless steel plates provides 4.5 tons of target in the fiducial volume. Thus  $\nu$  Nucleus interactions can be studied as well as  $\nu$  proton (or neutron) interactions. Moreover, no information about the  $\nu$  flux or radial distribution is needed to determine  $\sigma(n)/\sigma(p)$ .

H. Additional Features of the ITC system

1) Measurement of backgrounds

The non-neutrino backgrounds in the chamber can be measured accurately. One performs kinematic fits of  $H_2$  events to reactions\* such as  $np \rightarrow pp\pi^-$ ,  $K_L^0 p \rightarrow pK^\pm \pi^\mp$ ,  $\gamma p/e \rightarrow e^+e^- (p/e)$ . These fits can then be checked by observing the attenuation versus number of plates passed. This is especially important at high energy where ambiguities arise. In the  $\nu p$  bare chamber experiment (E45) these backgrounds were  $N_n/N_\nu$  (c.c.) =  $(1.4 \pm 1.0)\%$  and  $N_{K_L^0}/N_\nu$  (c.c.)  $\leq (1.2 \pm 1.2)\%$ ,  $N_\gamma/N_\nu$  (c.c.)  $< < 1\%$ .

2) Visual determination of x, y, z of points on tracks

At the points where the charged tracks enter each of the plates, one can determine the spatial coordinates approximately from inspection of view 1. Thus one can actually follow the dip of the track and one can see if the track begins in the  $H_2$ . This is

\* The inclusive reaction  $K_L^0 p \rightarrow K_S^0 X$  can also be used to set an upper limit on the  $K_L^0$  background.

-7-

especially important for single prong topologies which otherwise slow down scanning significantly.

3) Independence of  $\bar{\ell}_\gamma$  and  $\bar{\ell}_{\text{hadrons}}$

In H-Ne mixes and TST one cannot specify  $\bar{\ell}_\gamma$  and  $\bar{\ell}_{\text{hadrons}}$  independently because there is only one free parameter, the percent of Ne. However, with ITC there are two independent variables, the atomic number and thickness of the plates. Thus one can first select the effective number of radiation lengths for the chamber and then choose the hadronic mean free path within a factor of 30 (C to Pb). We chose stainless steel as a balance between cost,  $\bar{\ell}_{\text{hadrons}}$ , target tonage, and material strength.

### III. PHYSICS

#### A. Study of Di-lepton Production

The observation by the Harvard-Penn-Wisconsin-Fermilab and by the Caltech-Fermilab collaborations of neutrino-induced  $\mu^- \mu^+$  production and more recently by the Cern Gargamelle and Berkeley-Cern-Hawaii-Wisconsin groups of  $\mu^- e^+ K_S^0$  production in heavy nuclear targets has emphasized the importance of the weak interaction in new particle production. The proposed ITC experiment could provide a decisive understanding of these phenomena for the following reasons:

- 1) A di-lepton yield of approximately 1700 events is expected

-8-

- 2) Both charged and neutral hadrons are detected, as well as the leptons.
- 3) All types of associated strange particles ( $V^0$  and kink decays) can be studied.
- 4) The intrinsic mass resolution for new particle semi-leptonic decays is an order of magnitude better (i.e., 50-100 MeV vs. 500-1000 MeV) for the 0-c fit for free protons than for nuclei.

We now proceed to discuss in more detail the di-lepton channels.

- 1)  $\nu p \rightarrow \mu^- e^+ X$ . This channel (120 events) will be easy to detect because the electron detection efficiency at all momenta is  $> 95\%$  after measurement (an electron loses an average of 40% of its momentum in traversing a single plate). The total background in the  $\mu^- e^+ X$  sample from asymmetric Dalitz pairs, close-in  $\gamma$ 's, electrons from undetectable meson decays, etc. will be less than 2%. In this channel, one can study the  $E_\nu$ ,  $W$ (total hadronic mass),  $q^2$ ,  $X$ , and  $Y$  distributions as well as the details of the hadronic vertex such as charged and neutral multiplicity, and various effective mass combinations of the  $e^+$ ,  $\nu_e$  and hadrons. By examining mass combinations separately and cumulatively (e.g.,  $e^+ \nu_e K_S^0 + e^+ \nu_e K_S^0 \pi^+ \pi^- + \text{etc.}$ ) one should be able to isolate the new particle or particles whose semi-leptonic decay has been observed and measure branching ratios and other parameters.

- 2)  $\nu\text{Nuc} \rightarrow \mu^- e^+ X$ . The expected yield in this channel is 730 events. There is the problem of highly asymmetric electron pairs in the production plate which fake single positron production because the low momentum electron does not escape from the plate. Thus, approximately 4% of the charged current events will fake  $\mu^- e^+$ . Since this is four times the expected  $\mu^- e^+$  rate, something has to be done to reduce this background. This background can be reduced by an order of magnitude after calculating the effective mass of the  $e^+$  with other converted  $\gamma$ 's. One should still get  $m_{\pi^0}$  if the  $e^+$  came from a  $\pi^0$ . Then the background is 29% of the  $\mu^- e^+$  sample. The background can be further reduced to  $< 10\%$  rather easily by rejecting events with  $P_{e^+} < 1 \text{ GeV}/c$  with only a small loss in signal (based on E-28 results). Various other cuts can be made but will probably not be needed.
- 3)  $\nu p \rightarrow \mu^- \mu^+ X$  and  $\nu\text{Nuc} \rightarrow \mu^- \mu^+ X$ . Considering hadron punch-through (reduced a factor of two by hadron interactions in the plates) and other backgrounds in the EMI, about 3% of the charged-current events will appear to be  $\mu^- \mu^+$  events. If the  $\mu^- \mu^+ K_S^0 X$  and  $\mu^- e^+ K_S^0 X$  rates are equal, as expected, then the EMI-identified  $\mu^- \mu^+ K_S^0$  events should contain 15% background. Kinematic cuts can be made to reduce this background to less than 10%. A minimum  $P_{\mu^+}$  cut of  $2 \text{ GeV}/c$  may be needed to improve the EMI efficiency leaving a yield of about 400 events.

## B. New Particle Production

### 1) Charmed Particle Searches

From the basic quark transition amplitudes for:

- (i)  $\nu d \rightarrow \mu^- c$  ( $\sim \sin \theta_c$ )
- (ii)  $\nu s(+\bar{s}) \rightarrow \mu^- c(+\bar{s})$  ( $\sim \cos \theta_c$ )
- (iii)  $\nu \bar{c}(+c) \rightarrow \mu^- \bar{s}(+c)$  ( $\sim \cos \theta_c$ )
- (iv)  $\nu d(+c\bar{c}) \rightarrow \mu^- \nu(+c\bar{c})$  ( $\sim \cos \theta_c$ )

We would expect charmed particle production to proceed in various channels, such as:

$$\nu p \rightarrow \mu^- C^{++}, \nu n \rightarrow \mu^- C^+ \quad (1)$$

$$\nu p \rightarrow \mu^- D^+ p, \nu n \rightarrow \mu^- D^0 p \quad (2)$$

$$\nu p \rightarrow \mu^- K^0 C^{++}, \nu n \rightarrow \mu^- K^0 C^+ \quad (3)$$

$$\nu p \rightarrow \mu^- \bar{D}^0 C^{++}, \nu n \rightarrow \mu^- \bar{D}^0 C^+ \quad (4)$$

Single charm reactions such as (1)-(3) are allowed only in weak interactions; double-charm reactions such as (4) can be produced in any interaction. Reactions such as (1)-(2) of class (i) have strength  $\sim \sin^2 \theta_c$  and are off valance quarks. Thus, they should proceed with a total rate of a few percent of the total charged current rate producing about 2500 charged-current charmed particle events (for a 3% rate). Reactions such as (3) of class (ii) or (iii) have no Cabbibo suppression ( $\sim \cos^2 \theta_c$ ) but occur off sea quarks ( $s\bar{s}$  or  $c\bar{c}$ ) and are therefore more difficult to estimate. Most

theorists feel that  $s\bar{s}$  should dominate  $c\bar{c}$ . If reaction (3) is detected, the production dynamics will yield information on the relative strengths of  $s\bar{s}$  versus  $c\bar{c}$ . Assuming a rate of 0.5% one expects about 400 events of this type. Double-charm reactions such as (4) are not unique to the weak interaction and are not further discussed here except to point out that they are quite amenable to analysis in an ITC experiment.

Depending on the masses of the lowest-lying charmed states, the charmed particles would decay strongly to lower-lying charmed states or weakly hadronically or semi-leptonically. A comprehensive discussion of decay modes is given in Ref. 4 and elsewhere. An ITC experiment allows charmed (or other types of new) particles to be detected in several ways. In fact, it is difficult to imagine any type of decay mode to which the ITC is not sensitive. We now explain this in more detail.

a) Detection of stable particle decay products

The ITC can detect every type of stable particle except an outgoing neutrino. These are  $\gamma$ ,  $e^{\pm}$ ,  $\mu^{\pm}$ ,  $\pi^{\pm}$ ,  $\pi^0$ ,  $K^{\pm}$ ,  $K_S^0$ ,  $K_L^0$ ,  $\eta$ ,  $p$ ,  $n$ ,  $\Lambda$ ,  $\Sigma^{\pm}$ ,  $\Sigma^0$ ,  $\Xi^{-}$ ,  $\Xi^0$ , and  $\Omega^{-}$ .

b) Accessible effective mass combinations

Effective masses which include  $\gamma$ ,  $e^{\pm}$ ,  $\pi^0$ ,  $K_S^0$ ,  $K_L^0$ ,  $\eta$ ,  $\Lambda$ ,  $\Sigma^{\pm}$ ,  $\Sigma^0$ ,  $\Xi^{-}$ ,  $\Xi^0$ ,  $\Omega^{-}$  are straightforward and independent of constrained

-12-

production fitting because these particles are well identified and measured. For  $\mu^\pm$ ,  $\pi^\pm$ ,  $K^\pm$ , p the tracks are well measured but often ambiguous in nature. Several ways to overcome this problem exist. One can identify these particles by:

- (i) EMI and in-chamber interactions or decays to distinguish muons from hadrons.
- (ii) Kinematic production fitting for  $H_2$  events.
- (iii) Elastic scatters, kink decays ( $K^\pm$ ),  $(\pi\mu e)^\pm$  decays,  $(\mu e)^\pm$  decays, delta-rays, geometrical fitting and track residuals.

Furthermore, all tracks not identified otherwise can be taken as candidates for the desired mass hypothesis. Thus semi-inclusive  $\Lambda\pi^+\pi^+$  combinations, for example, can be formed with large statistics. This technique has been used in E-45 (vp) and easily identifies the  $\Sigma^+(1385) \rightarrow \Lambda\pi^+$ .

Neutrons have relatively low (~ 50%) detection efficiency. When the final state baryon is anything but a neutron, the momentum is relatively well measured otherwise it is relatively poorly known.

For decays with one neutrino, one has the 0-c fit. It is even possible to see mass peaks from decays involving two or more neutrinos. For example  $vp \rightarrow \mu^-\xi^{++}$  followed by  $\xi^{++} \rightarrow$  possible hadrons + possible charged leptons + two neutrinos.

One can see a peak in the W-distribution (mass resolution  $\sim 200-500$  MeV) by using the Myatt solution for  $E_\nu$ .

We recall that charmed decays often produce  $\Delta S/\Delta Q$  violations which aids in their detection since exotic quantum numbers are needed:  
e.g.,  $C^{++} \rightarrow \Lambda \pi^+ \pi^+$ ,  $D^+ \rightarrow K^- \pi^+ \pi^+$ , etc.

One would also expect diffractive production of charmed vector mesons via the weak charged current; for example  $F^*$  production in

$$\nu p \rightarrow \mu^- F^{*+} p. \quad (5)$$

The diagram for this reaction is shown in Fig. 4a. The  $F^*$  would probably decay electromagnetically to a charmed pseudoscalar meson:

$$F^{*+} \rightarrow F^+ \gamma. \quad (6)$$

The  $F^+$  then would presumably decay weakly to hadronic ( $\pi^+ \pi^+ \pi^-$ ,  $K^+ \bar{K}^0$ ,  $\eta \pi^+$ , etc.), leptonic and semi-leptonic ( $\ell^+ \nu$ ,  $\eta \ell^+ \nu$ , etc.) final states.

A signature for  $F^*$  production is single  $\gamma$  production and correlated peaks in, for example,  $\pi^+ \pi^+ \pi^-$  (F) and  $\pi^+ \pi^+ \pi^- \gamma$  ( $F^*$ ).

2) Diffractive  $\psi$  Production by Weak Neutral Current

The diffractive production of  $\psi(3100)$  and  $\psi(3700)$  via

$$\nu p \rightarrow \nu \psi p \tag{7}$$

(Figure 4b) should proceed with strength comparable to reaction (3). Reaction (7) provides information on  $Z^0$  quantum numbers and on  $Z^0 - \psi$  coupling and could be the dominant reaction for  $\psi$  production by neutrinos. The need for good charged lepton and  $\pi^0$  identification and measurement is apparent here.

3) Heavy Lepton Production

A charged heavy lepton with the normal  $\mu$ -lepton (or  $e$ -lepton) number could decay electromagnetically by

$$\mu^* \rightarrow \mu \gamma \tag{8a}$$

$$e^* \rightarrow e \gamma \tag{8b}$$

with  $\tau \sim 10^{-21}$  sec.<sup>5</sup> or via

$$\mu^* \rightarrow \mu + \text{hadrons.} \tag{9a}$$

$$e^* \rightarrow e + \text{hadrons} \tag{9b}$$

On the other hand, there may exist heavy leptons with new lepton numbers which decay like

$$L \rightarrow \ell \bar{\nu}_\ell \nu_L \quad (10)$$

where  $\ell = \mu$  or  $e$ , or like

$$L \rightarrow \nu_L + \text{hadrons.} \quad (11)$$

Neutral heavy lepton (heavy neutrino) production by neutrinos can also occur. We again distinguish between old lepton number:

$$\nu_\mu^* \rightarrow \nu_\mu \mu^+ \mu^- \quad (12)$$

$$\rightarrow \nu_\mu e^+ e^- \quad (13)$$

$$\rightarrow \mu^- e^+ \nu_e \quad (14)$$

$$\rightarrow \nu_\mu X \quad (15)$$

$$\rightarrow \mu^- X \quad (16)$$

and new lepton number:

$$\nu_L \rightarrow LX \text{ (if } M_{\nu_L} > M_L) \quad (17)$$

$$\rightarrow \text{stable, otherwise?} \quad (18)$$

To detect and study heavy leptons we see again the need for good charged lepton and  $\gamma$  identification and measurement.

4) Intermediate Vector Boson Production

Above threshold one expects charged IVB production from the reaction

$$\nu p \rightarrow \mu^- W^+ p \quad (19)$$

The lowest order diagrams for reaction (19) shown in Fig. 4c, d have been calculated in Ref. 6. Since  $W^+$  decays to  $\mu^+ \nu$  the final state for reaction (19) is  $\nu \mu^- \mu^+ p$ . The signature for this reaction is then a  $\mu^+ \mu^-$  pair, p imbalance but no  $\pi^0$ . Furthermore one expects  $p_{\mu^-}$  to be small and  $p_{\mu^+}$  large. We note that once  $\pi^0$  production has been vetoed it is possible to perform a (0-c) fit to reaction (19) and thus measure the mass of the IVB to about 5% accuracy. Current experimental and theoretical results make it doubtful that IVB production can proceed at presently available accelerator energies, however.

##### 5) Production of Other New Particles

We briefly comment here on the relevance of the ITC system to the detection of other hypothetical particles, such as quarks or magnetic monopoles. Although it is currently fashionable to think of quarks as light, totally-confined constituents rather than heavy objects awaiting emancipation, it is nevertheless important to be on the alert for their production. It would appear that hydrogen is the best detector. Quark signatures are (i) apparent charge-nonconservation since they have fractional charges, (ii) less than minimum (4/9, 1/9) ionization, (iii) less than minimum energy loss. Regarding (i), hydrogen is the only liquid in which the observed final state charge is unique. It further appears that H-Ne mixes give no ionization information in the 15-ft. chamber. (ii)

Energy losses in H-Ne mixes are larger but the ITC largely compensates for this (iii) The general advantage of ITC is better overall understanding of the final state in which possible quark production arises.

Magnetic monopoles are detected in a bubble chamber from the coincidence between their drift paths and the chamber magnetic field lines since their initial energy is quickly dissipated. The large transverse multiple scattering in the plates could lead to further identification.

### C. Measurement of $\sigma(n)/\sigma(p)$ for Charged and Neutral Currents

From measurements of relative production rates for charged and neutral currents on two types of target containing different and known ratios of protons and neutrons, one determines  $\sigma(n)/\sigma(p) = \eta$ . The ITC system with hydrogen is especially well suited to measure  $\eta_{CC}$  and  $\eta_{NC}$  because:

- (i) The target (p or nucleus) is always identified because the targets are spatially separated. In  $D_2$  there is an uncertainty of ~5% as to whether a proton or neutron was struck due to higher order diagrams. In H-Ne mixes, the uncertainty is much higher.
- (ii) Both the absolute flux and the radial flux distributions cancel in ITC determinations\* of  $\eta_{NC}$  and  $\eta_{CC}$ . The radial flux distribution does not cancel in TST

---

\* Various other systematic errors also cancel: scanning, reconstruction efficiencies and, to some extent, even backgrounds.

except directly downstream of the hydrogen where the available volume is small, tracks are short, making neutrino energy estimation difficult, and  $\gamma$  detection is lower.

Yields for both  $H_2$  and nuclear interactions are given in Table I. The errors in  $\eta_{cc}$  and  $\eta_{nc}$  come primarily from the statistical error in the number of  $H_2$  events and from the cc/nc separation. Folding these together, we expect errors to be  $\sim 2\%$  for both  $\eta_{cc}$  and  $\eta_{nc}$  neglecting contributions from channels hard to detect and identify like  $\nu_n \rightarrow \nu_n$ .

At present  $\eta_{cc}$  is known to about 15% at low energy and  $\eta_{nc}$  is unknown.

Finally, we note that there is a simple relation between  $\eta_{cc}$ ,  $\eta_{nc}$  and the nc to cc ratios  $R_n$  and  $R_p$  namely

$$\eta_{nc}/\eta_{cc} = R_n/R_p. \quad \text{Eq. (1)}$$

#### D. Deep Inelastic Scattering

Considerable effort in recent years has gone into theoretical and experimental studies of deep inelastic neutrino scattering. Measurements of the weak structure functions compare favorably with predictions of quark parton models. Both virtual W-bosons in neutrino scattering and virtual photons in electroproduction probe and provide information on the elementary quarks; however W-bosons couple to quarks of a given type whereas photons couple to all quarks. Thus, one can learn more about the properties of individual quarks from deep inelastic neutrino scattering.

1) Charged Current Reactions

From a combination of EMI data, plate penetration and transverse momentum considerations (with almost all hadronic energy materialized) we can identify 96% of charged current events. Since the hadron energy is known to ~8%,  $E_\nu$  is known to ~4%. Using a  $p_t$  balance procedure<sup>7</sup> we can reduce the error on  $E_\nu$  to ~2%.

One can measure  $W$ ,  $q^2$ ,  $\nu$ ,  $x$ ,  $y$  better than in a bare  $H_2$  chamber. Table II shows a comparison of the resolution which can be obtained in bare  $H_2$  and ITC with  $H_2$ . Since the resolution in  $W$  is about four times better, one has 2 times as much sensitivity (4 times less background) in searching for narrow (charmed?) baryon states which have neutrals among their decay products.

Deep inelastic studies can be made on protons and nuclei simultaneously. One can then isolate the effects in any distribution ( $q^2$ ,  $\nu$ ,  $x$ ,  $y$ , etc.) caused by p or n. Nuclear effects will have to be unfolded, however. From  $\langle q^2 \rangle$  vs.  $E_\nu$  one can measure, or set a lower limit on, the  $W$ -propagator mass. From the mean charge of the current fragments in the Breit frame or, alternately from the positive and negative particle  $Z = E/\nu$  distributions one can effectively measure the u-quark charge. Results on these last two items will come from the bare chamber  $H_2$  experiment (E-45), but more precise results will be

obtained with ITC because the cc-nc separation is cleaner and  $E_\nu$  is better determined.

Of course, the improved resolution in x, y will enable one to see more easily any anomalies in their distributions.

2) Neutral Current Reactions

From the non-observation of a muon plus the  $p_t$  procedure (with almost all hadronic energy visible) one can identify ~95% of the nc events. Neutron and  $K_L^0$  backgrounds will then have to be subtracted. Then by Monte-Carlo corrections, with checks provided by the real data, we can find the true number of nc and cc events to ~2 percent. The neutrino energy for nc events can be estimated from the equation:

$$E_\nu = \frac{M_H^2 + M_p^2 - 2 M_p E_H}{2(E_H - P_H \cos\theta_H - M_p)} \quad \text{Eq. (2)}$$

Thus we must estimate  $E_H$ ,  $P_H$  and  $\theta_H$ . To do this we must know what fraction of hadronic energy is visible on the average. Since the average  $\gamma$  conversion efficiency is 0.9 and ~1/3 of the mesons are  $\pi^0$ 's, then ~0.97 of the mesonic energy is visible. Furthermore about 0.5 of the neutrons will interact in the plates or  $H_2$ . Since ~1/2 of the outgoing nucleons are neutrons, ~0.75 of the nucleonic energy is visible. The average number of charged hadrons is 4 and the average number of  $\pi^0$ 's is

2. Then the average fraction of total hadronic energy visible is 0.90. It then appears that we can say that  $\theta_H \approx \theta_H$  (visible) and  $P_H \approx P_H$  (visible)/0.9. The difficulty arises in estimating  $E_H$ . First one must assign masses,  $\{m_i\}$ , to the charged prongs. Since negatives are almost always pions, this presents no problem. For positives with  $p \lesssim 1.5$  GeV/c the geometry program usually distinguishes between p and  $\pi$ . For positives with  $P \gtrsim 1.5$  GeV/c the best one can do is first assume all are  $\pi$ 's, then cycle the proton interpretation among the tracks to set bounds on  $E_H$  (visible). The main problem lies in estimating  $E_H$  (invisible). Do we have no neutrals, a neutron, one or more  $\gamma$ 's or  $n + \gamma$ 's missing? Since there is no good way to do this on an event by event basis - there might be a good overall correction based on a statistical procedure - the best one can probably do is to take  $E_H$  (total)/ $E_H$  (visible) =  $P_H$  (total)/ $P_H$  (visible) = 1/0.9. A preferable method appears to exist. We observe from Table III that if an even number of primary  $\gamma$ 's materialize, the probability is very high, 0.93 on the average, that all  $\gamma$ 's have converted. Coupled with the neutron interaction probability, the probability that all hadronic momentum is visible in these events is 0.70. There is a 0.30 probability that a small fraction, 0.20, of the hadronic momentum is missing. Thus one applies Eq. (2) directly to all even  $\gamma$  events with  $E_H$ ,  $P_H$ ,  $\theta_H$  given by their visible counter parts.

The small error from the missing neutrons can be corrected from the neutron-star events. The even smaller error from the 2 missing  $\gamma$  events can be corrected from the charged current events with neutron-stars since then one knows whether 0 or 2  $\gamma$ 's are missing. Various other methods exist which could prove to be even better than this one.

It thus appears that we can measure neutral-current  $E_\nu$ ,  $x$ ,  $y$ ,  $q^2$ ,  $\nu$ ,  $W$ , etc. distributions on protons and possibly on nuclei as well. Table II shows the expected resolution on these variables from a Monte-Carlo with experimental resolution folded in.

E. Exclusive Channels

Charged current exclusive channels with no missing neutrals, such as  $\mu^- p \pi^+$ , give 3-constraint fits and can be done quite well in a bare  $H_2$  chamber. The advantages of ITC are (i) charged current channels with  $\pi^0$ 's and/or neutrons can be fit, (ii) neutral current channels with or without  $\pi^0$ 's can be identified and fit (0-c fit) when identifiable protons or measurable neutron-stars are present.

1) Resonance Production

a) Meson Resonances

We will compare  $\rho$  diffractive production in charged and neutral current channels:

$$\nu p \rightarrow \mu^- \rho^+ p \quad (20)$$

$$\nu p \rightarrow \nu \rho^0 p \quad (21)$$

The diagrams for these channels are shown in Fig. 4e, f.

From the measured distributions we learn about  $W^+ - \rho^+$  and  $Z^0 - \rho^0$  coupling in a vector dominance model. Since both final states contain one neutral, it is important to rule out additional  $\pi^0$ 's.

The neutral current reaction:

$$\nu p \rightarrow \nu \omega^0 p \quad (22)$$

is also accessible for study. Channels which include other meson resonances such as  $\eta$ ,  $\eta'$ ,  $\phi$ ,  $A_2$ ,  $f$  are possible.

#### b) Baryon Resonances

Studies of baryon resonance production can be made in the following reactions:

$$\nu p \rightarrow \mu^- \Delta^{++} \quad (23)$$

$$\rightarrow \nu \Delta^+ \quad (24)$$

$$\rightarrow \nu N^+ \quad (25)$$

#### c) Double Resonance Production

And finally we list some double resonance channels which are accessible:

$$\nu p \rightarrow \mu^- \rho^0 \Delta^{++} \quad (26)$$

$$\rightarrow \mu^- \omega \Delta^{++} \quad (27)$$

$$\rightarrow \nu \rho^- \Delta^{++} \quad (28)$$

$$\rightarrow \nu \rho^0 \Delta^+, N^+ \quad (29)$$

$$\rightarrow \nu \rho^+ \Delta^0, N^0 \quad (30)$$

## 2) Strange Particle Production

Strange particle production is important because it provides information on charm production, selection-rules and further properties of the weak charged and neutral currents.

### a) charged currents

#### (i) $\Delta S = 0$

Associated production reactions accessible are:

$$\nu p \rightarrow \mu^- \Lambda K^+ \pi^+ M^\dagger \quad (31)$$

$$\rightarrow \mu^- \Sigma^+ K^+ M \quad (32)$$

$$\rightarrow \mu^- \Sigma^0 K^+ \pi^+ M \quad (33)$$

$$\rightarrow \mu^- \Sigma^- K^+ \pi^+ \pi^+ M \quad (34)$$

$$\rightarrow \mu^- \Xi^- K^+ K^+ \pi^+ M \quad (35)$$

$$\rightarrow \mu^- \Xi^0 K^+ K^+ M \quad (36)$$

$$\rightarrow \mu^- p K^+ \bar{K}^0 M \quad (37)$$

$$\rightarrow \mu^- p K^- K^0 M \quad (38)$$

---

$M^\dagger$  stands for nothing or any combination of  $\pi^+ \pi^-$  pairs and  $\pi^0$ 's.

-25-

In these, and all following reactions  $K^+(K^-)$  can also be taken as  $K^0\pi^+(\bar{K}^0\pi^-)$

$$(ii) \quad \underline{\Delta S = \Delta Q}$$

These reactions are a measure of the  $q-\bar{q}$  sea content of the nucleon, i.e.,

$$\nu\bar{u} \rightarrow \mu^- \bar{s} + \text{left-over } u \quad (\sim \sin \theta_c)$$

$$\nu s \rightarrow \mu^- u + \text{left-over } \bar{s} \quad (\sim \sin \theta_c)$$

and lead to

$$\nu p \rightarrow \mu^- p K^+ M \quad (39)$$

$$\rightarrow \mu^- n K^+ \pi^+ M \quad (40)$$

$$\rightarrow \mu^- \bar{\Lambda} p p M \quad (41)$$

Even though these reactions are doubly-suppressed by (sea content and Cabbibo angle) a total of about 50 events is expected.

$$(iii) \quad \underline{\Delta S = -\Delta Q.}$$

Reactions of this type are of great significance. They imply either  $\Delta S/\Delta Q$  violating currents or charm production. Examples of  $\Delta S = -\Delta Q$  reactions are:

$$\nu p \rightarrow \mu^- \Lambda^0 \pi^+ \pi^+ M \quad (42)$$

$$\rightarrow \mu^- \Sigma^+ \pi^+ M \quad (43)$$

$$\rightarrow \mu^- \Sigma^0 \pi^+ \pi^+ M \quad (44)$$

$$\rightarrow \mu^- \Sigma^- \pi^+ \pi^+ \pi^+ M \quad (45)$$

$$\rightarrow \mu^- p K^- \pi^+ \pi^+ M \quad (46)$$

An example of reaction (42) has been published<sup>8</sup> but is so far unconfirmed.

b) neutral currents

(i)  $\Delta S = 0$

Associated production is believed to be the only kind of strangeness reaction allowed.

Practically nothing is known about neutral current induced strange final states, such as

$$\nu p \rightarrow \nu \Lambda K^+ M \quad (47)$$

$$\rightarrow \nu \Sigma^+ K^0 M \quad (48)$$

$$\rightarrow \nu \Sigma^0 K^+ M \quad (49)$$

$$\rightarrow \nu \Sigma^- K^+ \pi^+ M \quad (50)$$

(ii)  $\Delta S = \pm 1$

Observation of reactions of the type:

$$\nu p \rightarrow \nu K^0 p M \quad (51)$$

$$\rightarrow \nu \Lambda \pi^+ M \quad (52)$$

$$\rightarrow \nu \Sigma^+ M \quad (53)$$

$$\rightarrow \nu \Sigma^0 \pi^+ M \quad (54)$$

$$\rightarrow \nu \Sigma^- \pi^+ \pi^+ M \quad (55)$$

would not only violate the  $\Delta S = \Delta Q$  rule but would remove one of the main underpinnings of the charm theories:

the absence of strangeness - changing neutral currents.

Upper limits on these reactions will also be of value.

#### F. Heavy Particle Production from Nuclei

In addition to the results which can be obtained on deep inelastic scattering of neutrinos on heavy nuclei, neutrino-nucleus scattering may be an important source of heavy particle production. Except for coherent scattering - which, incidentally, can occur in neutral current reactions - short-lived ( $\tau \sim 10^{-23}$  sec) resonances produced in nuclei are difficult to detect because they decay inside the nucleus and their decay products then further interact.\* However, longer-lived particles such as lower-lying charmed particles, heavy leptons,  $\psi$ -particles (if they are not related to charm) can all be expected to decay outside the nucleus and are amenable to detection. The higher yields, availability of both p and n targets, plus possible coherent effects in nuclear interactions might be important in heavy particle production. The improved charged lepton and  $\gamma$  detection in ITC will also be of great help in searches for these and other particles.

\* Decays to  $\mu^+ \mu^-$ , e.g., are exceptions

### G. Pure Leptonic Interactions

The  $\nu_\mu e^-$  reactions in the hydrogen of the type:

$$\nu_\mu e^- \rightarrow \mu^- \nu_e \quad (56)$$

$$\rightarrow \nu_\mu e^- \quad (57)$$

(Figure 1e, f) should be detectable. Backgrounds from reactions on protons in which two positive charges are lost are negligible. Background to reaction (57) from  $\nu_e e^- \rightarrow \nu_e e^-$  will be small (since the  $\nu_e$  flux is 3 orders of magnitude smaller than the  $\nu_\mu$  flux) unless the cross section is anomalously large. There is no way to separate these reactions.

The advantages of ITC are (i) single negative prongs originating in the liquid will usually be identifiable in view #1 alone, (ii)  $\mu^-$  can be discriminated from  $e^-$  on the scan table via electron bremsstrahlung, (iii) possible additional  $\pi^0$  production can be vetoed on the scan table or after reconstructing any  $\gamma$ 's.

One expects roughly twice the yield of reactions (56) and (57) from electrons in the plates but this class of events will be more difficult to extract from the backgrounds of asymmetric pair production and/or bremsstrahlung of the low energy electron. An excess of fast single negative electrons above fast single positive electrons would indicate that these channels are accessible. Compton scattering cross sections for electron energies  $> 10$  GeV are completely negligible. In general, backgrounds from any  $\gamma$ -induced reaction can be identified by the characteristic attenuation through the chamber.

#### H. Charged and Neutral Particle Multiplicity Distributions

Distributions of interest are charged, neutral and total multiplicity distributions versus  $E_\nu$ . One would also like to measure  $\langle n_{+-} \rangle$ ,  $\langle n_0 \rangle$ ,  $\langle n_{+0-} \rangle$  vs.  $W^2$  and  $q^2$  and make comparisons with electroproduction and photoproduction data. Charged particle distributions are being obtained in the bare  $H_2$  experiment (E45). This experiment would improve the measurement of  $E_\nu$ ,  $W^2$  and  $q^2$  and allow neutral particle distributions to be measured as well.

REFERENCES

- <sup>1</sup>Bethe and Heitler, Proc. Roy. Soc., A146 (1934) 83.
- <sup>2</sup>Mo and Tsai, Rev. Mod. Phys., 41 (1969) 205.
- <sup>3</sup>Myatt, G. (unpublished).
- <sup>4</sup>Gaillard, Lee, Rosner, Rev. Mod. Phys., April (1975).
- <sup>5</sup>Low, F. E., Phys. Rev. Lett. 14 (1965) 238.
- <sup>6</sup>Brown and Smith, Phys. Rev. D3 (1971) 207; Brown, et al., Phys. Rev. Lett. 25 (1970) 257.
- <sup>7</sup>Burmeister and Cundy (unpublished).
- <sup>8</sup>Cazzoli, E. G., et al., Phys. Rev. Lett. 34 (1975) 1125.

TABLE I  
 YIELDS OF NEUTRINO EVENTS INSIDE  
 FIDUCIAL VOLUME FOR ITC  
 (based on E45 measurements)

Reaction	Number of Events*
$\nu_p \rightarrow \mu^- X$	12,000
$\nu_p \rightarrow \nu X$	3,000 <sup>†</sup>
$\nu_p \rightarrow \Lambda X$	600 <sup>‡</sup>
$\nu_p \rightarrow K_S^0 X$	600 <sup>‡</sup>
$\nu_p \rightarrow \mu^- e^+ X$	120
$\nu_p \rightarrow \mu^- \mu^+ X$	120
TOTAL $\nu_p$	15,000
$\nu_{Nuc} \rightarrow \mu^- X$	73,000
$\nu_{Nuc} \rightarrow \nu X$	12,000
$\nu_{Nuc} \rightarrow \mu^- e^+ X$	730
$\nu_{Nuc} \rightarrow \mu^- \mu^+ X$	730
TOTAL $\nu_{Nuc}$	85,000
$\nu_\mu e^- \rightarrow \mu^- \nu_e$	~40 (~120 <sup>#</sup> )
$\nu_\mu e^- \rightarrow \nu_\mu e^-$	~50 (~150 <sup>#</sup> )
TOTAL $\nu_\mu e$	90 (270 <sup>#</sup> )
TOTAL NEUTRINO EVENTS	100,000

\* 300K pictures,  $1.3 \times 10^{13}$  ppp, 400 GeV/c protons, 2 horns, 16 m<sup>3</sup> fid. vol.,  $\Sigma P_x$  (vis.) > 9 GeV/c.

<sup>†</sup>  $\Sigma P_x$  (vis.) > 5 GeV/c for neutral current events.

<sup>‡</sup> charged (i.e., visible) decays only.

<sup>#</sup> including events from plates.

TABLE III

CONVERSION PROBABILITY VERSUS NUMBER OF  $\gamma$ 's CONVERTED IF SINGLE  
 $\gamma$  CONVERSION PROBABILITY IS 0.9

PROB. TO CONVERT N PAIRS				
$N_{\gamma}$	$N = N_{\gamma}$	$N = N_{\gamma} - 1$	$N = N_{\gamma} - 2$	$N = N_{\gamma} - 3, N_{\gamma} - 4 \dots 0$
0	1.0	---	---	---
2	.810	.180	.010	---
4	.656	.292	.049	.003
6	.531	.354	.098	.017
8	.430	.382	.149	.039
10	.349	.387	.193	.071

## APPENDIX A

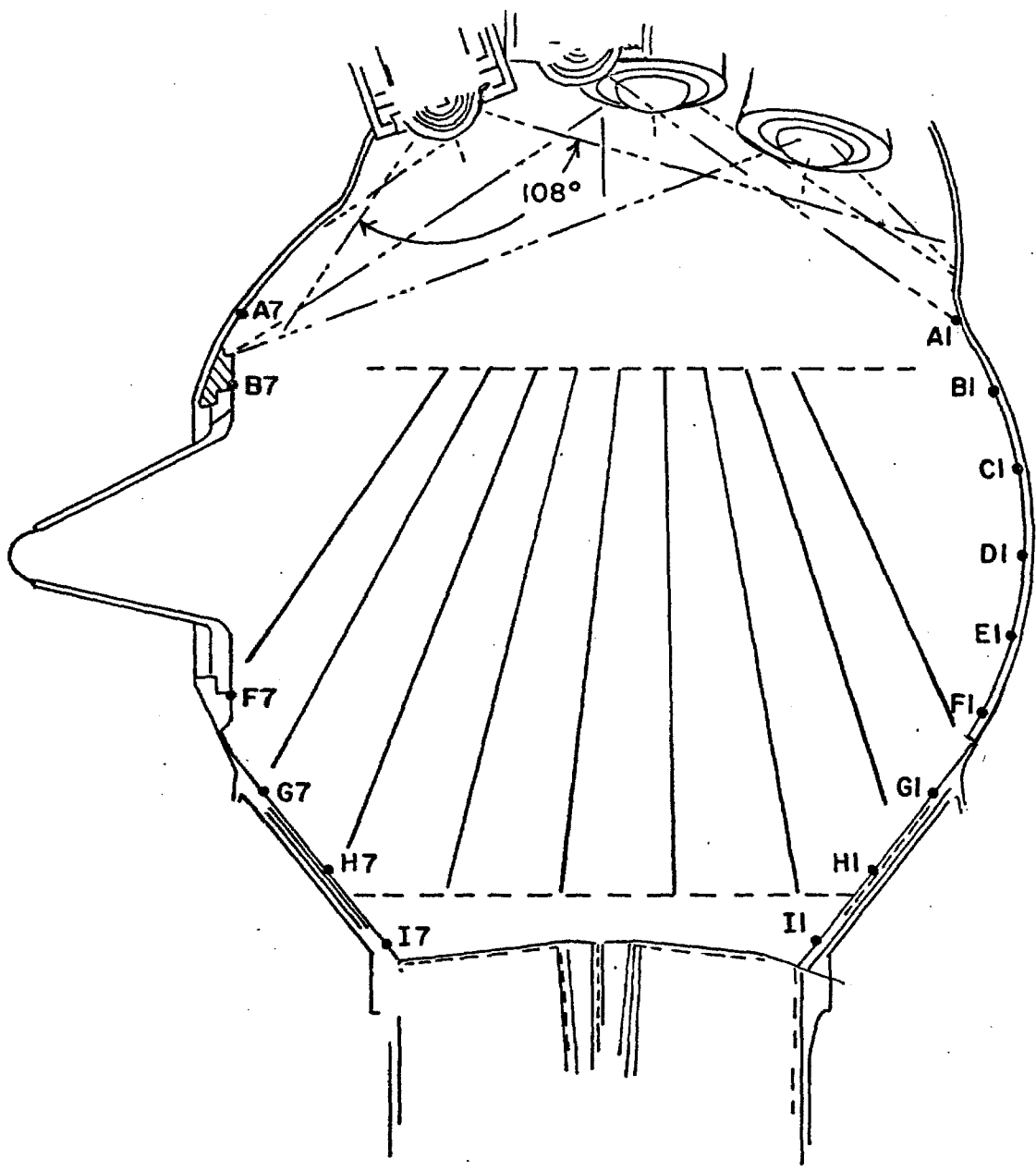
## Details of the ITC

(1) Construction: Each plate will be 0.9 cm thick and have radius 3-6" less than the chamber section at the corresponding place to allow for liquid circulation. The top of each plate will terminate at the plane given by  $Z = 70$  cm. If deemed advisable, a 4" x 18" rectangular hole will be cut in the center of each plate for a hadron beam window for possible ITC hadron experiments. Also a small (approximately 6" x 24") rectangular slot will be cut at the bottom of plates #2, #3, #7 and #8 as a manway for additional welding between in-place plates. These two sets of openings will reduce the area and mass of the plates by less than 1%. Since the piston port will not allow a plate with minimum dimension more than 6 ft. to pass through, plates #2-8 will each be installed in two half sections which may either be joined or else separated by a few centimeters. To allow visibility in View #1, the upstream surface of each plate will be chrome plated and possibly overcoated with silicon dioxide. Scotchlite strips will be put on the uppermost edge of each plate to render them almost invisible in Views #5 and 6. This will facilitate scanning and will allow plate numbers and additional fiducial crosses to be inked on. Each plate section will be mounted on brackets which have been pre-welded on the chamber wall.

(2) Boiling Considerations: Many experiments with plates show that negligible boiling occurs around the plates as long as edges are smooth, small crevices are absent and conditions resulting in high local velocities of the liquid are eliminated.

For example, the BNL 7 ft. chamber has run successfully with four large area plates closely spaced and has exhibited almost no boiling.

(3) Mechanical Strength: If stress analyses show that excessive flexing of the plates occurs during expansion, three different solutions exist. (i) use a lower Z material such as Ti, which would then require 1.8 cm thick plates, (ii) weld 1" diam. stainless steel rods as a bridge from plate to plate, (iii) suspend the plates on heavy springs at each bracket so the plates will move an inch with the liquid.



15-FT. CHAMBER WITH ITC  
(side view)

FIG. 1(a)

## APPENDIX B

Comparison of ITC, Downstream Plates (DP), TST and H-Ne.

Parameter	ITC	DP	TST	H-Ne (atomic)	
				20%	100%
Ave. $\gamma$ detection efficiency	90%	90%	90%	70%	99%
$\delta P/P$ for $\pi^0$ (before fitting) *	17%	>20%	8%	6%	10%
H <sub>2</sub> fiducial volume (m <sup>3</sup> )	16	~10	~3	-	-
Heavy nucleus fiducial mass (tons)	4.5	-	~15	5.2	26
Ability to measure $\sigma(n)/\sigma(p)$	exc.	poor	good	poor	poor
Ability to study $V^0$ decays	exc.	exc.	exc.	exc.	good
Ability to study kink decays	exc.	exc.	exc.	poor	poor
$\mu$ detection efficiency (>2 GeV)	>95%	>95%	>95%	>95%	>95%
e detection efficiency (after measurement)	>95%	>90%	>95%	>95%	>97%

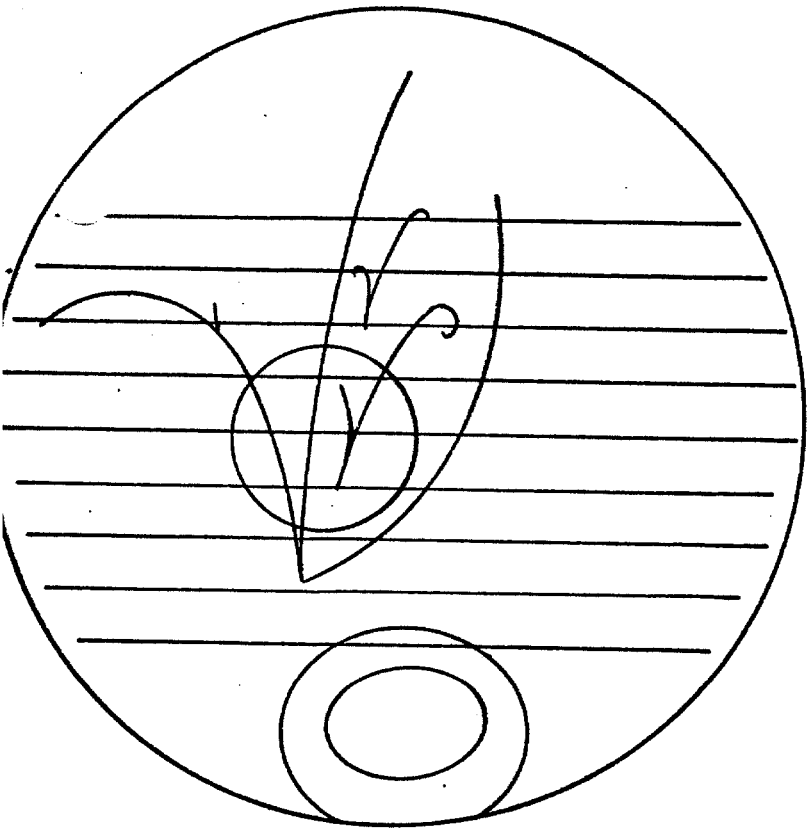
\* without using brem  $\gamma$ 's

TABLE II  
 RESOLUTION FOR BARE H<sub>2</sub> CHAMBER AND FOR ITC  
 WITH H<sub>2</sub>

Variable	Charged current events		Neutral current events	
	Bare H <sub>2</sub>	ITC + H <sub>2</sub>	Bare H <sub>2</sub>	ITC + H <sub>2</sub> *
E <sub>v</sub>	~8%	~2%	unmeasurable	~20%
x	~.03	~.007	"	~0.1
y	~.04	~.01	"	~0.1
q <sup>2</sup>	~8%	~2%	"	~20%
v	~16%	~4%	"	~ 5%
W	~8%	~2%	"	~ 7%

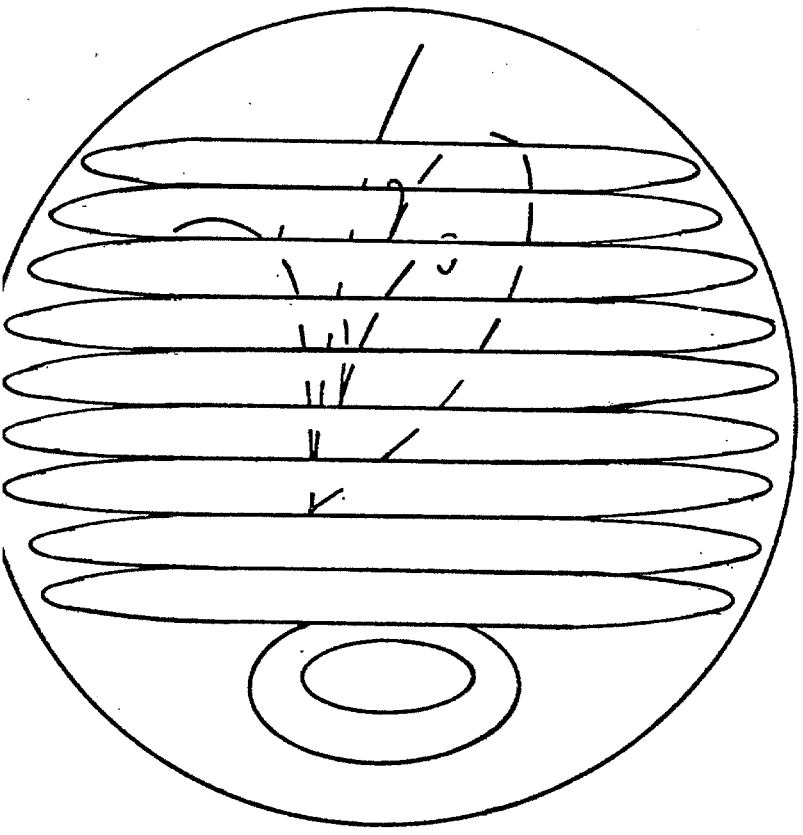
Note: Numbers quoted as percentages are fractional resolutions and decimal numbers are absolute resolutions

\* For final states with measurable baryons such as p,  $\Lambda$ ,  $\Sigma$ ,  
 np  $\rightarrow$  pp $\pi^-$ , etc.

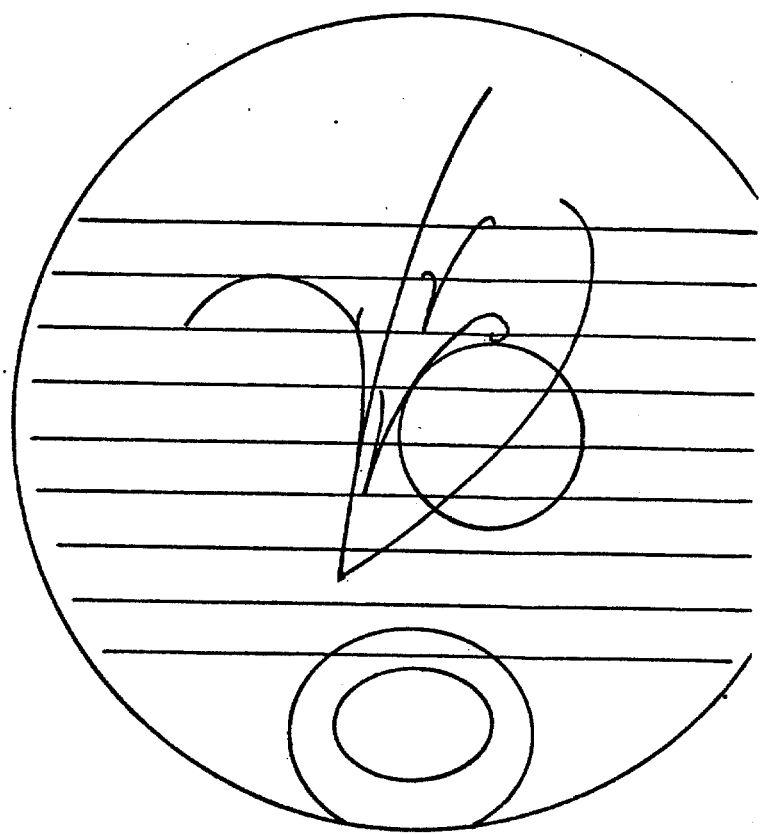


VIEW 5

3 - PRONG +  $\pi^0$



VIEW 1



VIEW 6

FIG. 1(b)

$\gamma$  CONVERSION PROB.

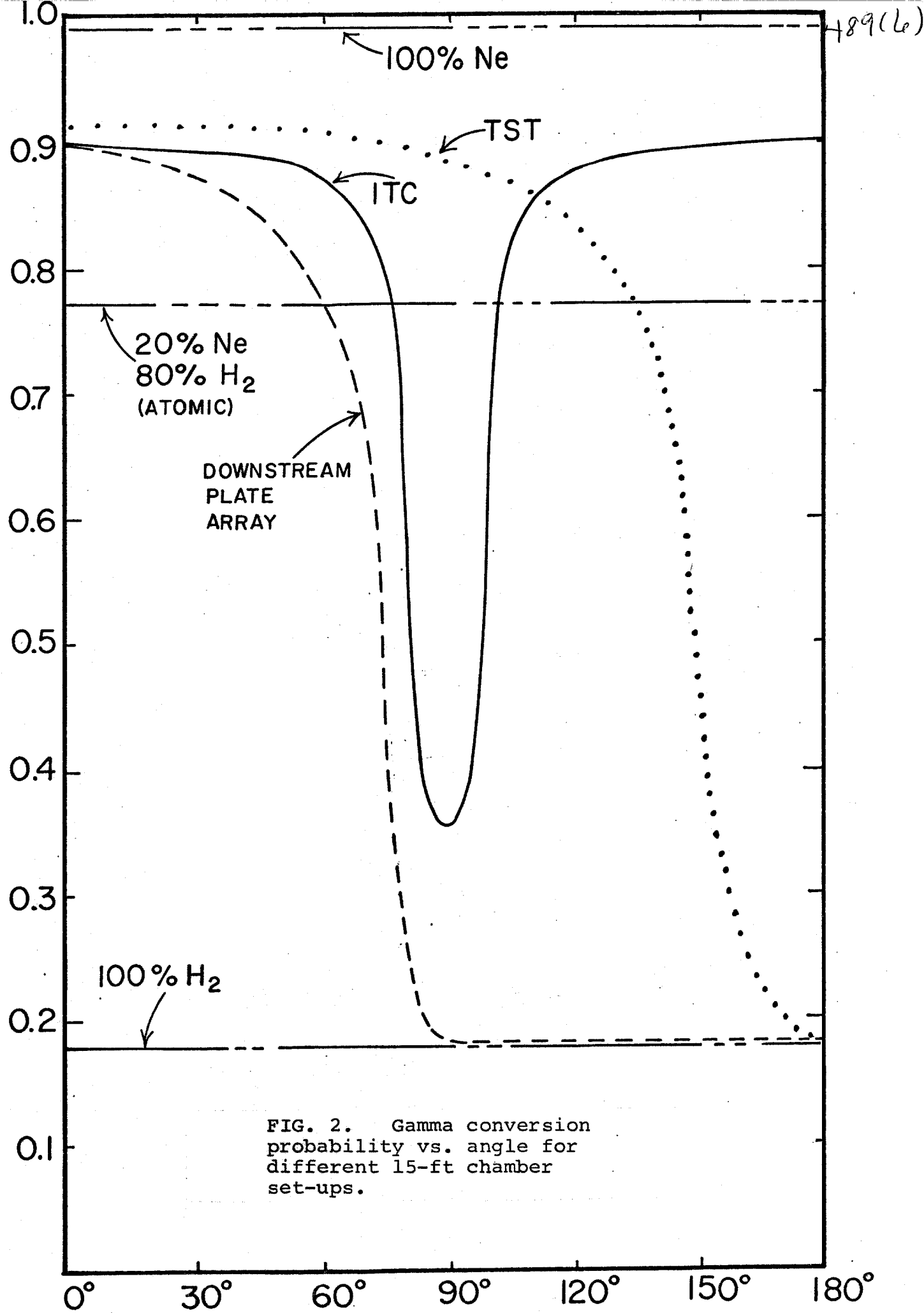


FIG. 2. Gamma conversion probability vs. angle for different 15-ft chamber set-ups.

$$\phi(\alpha, t)$$

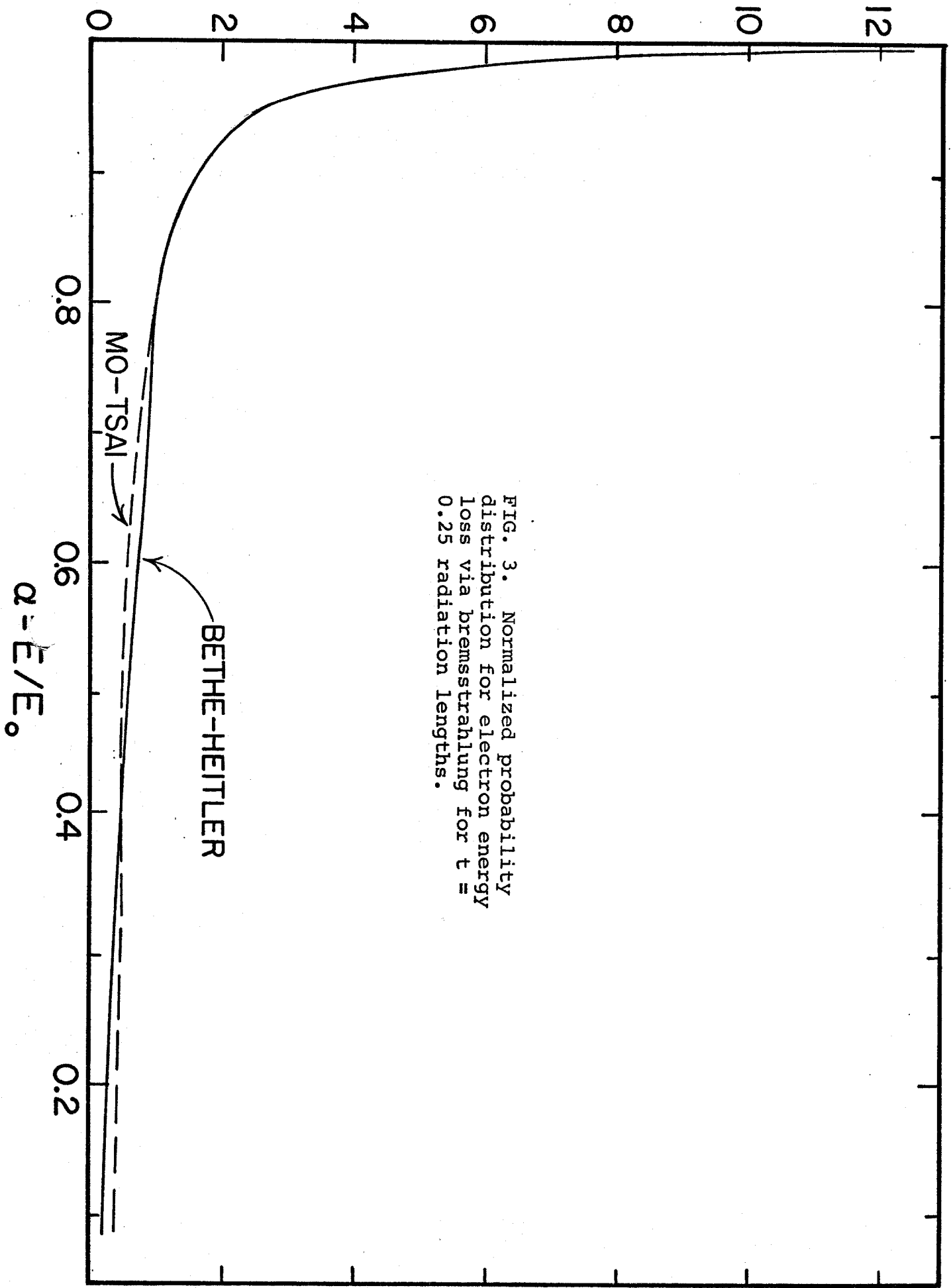
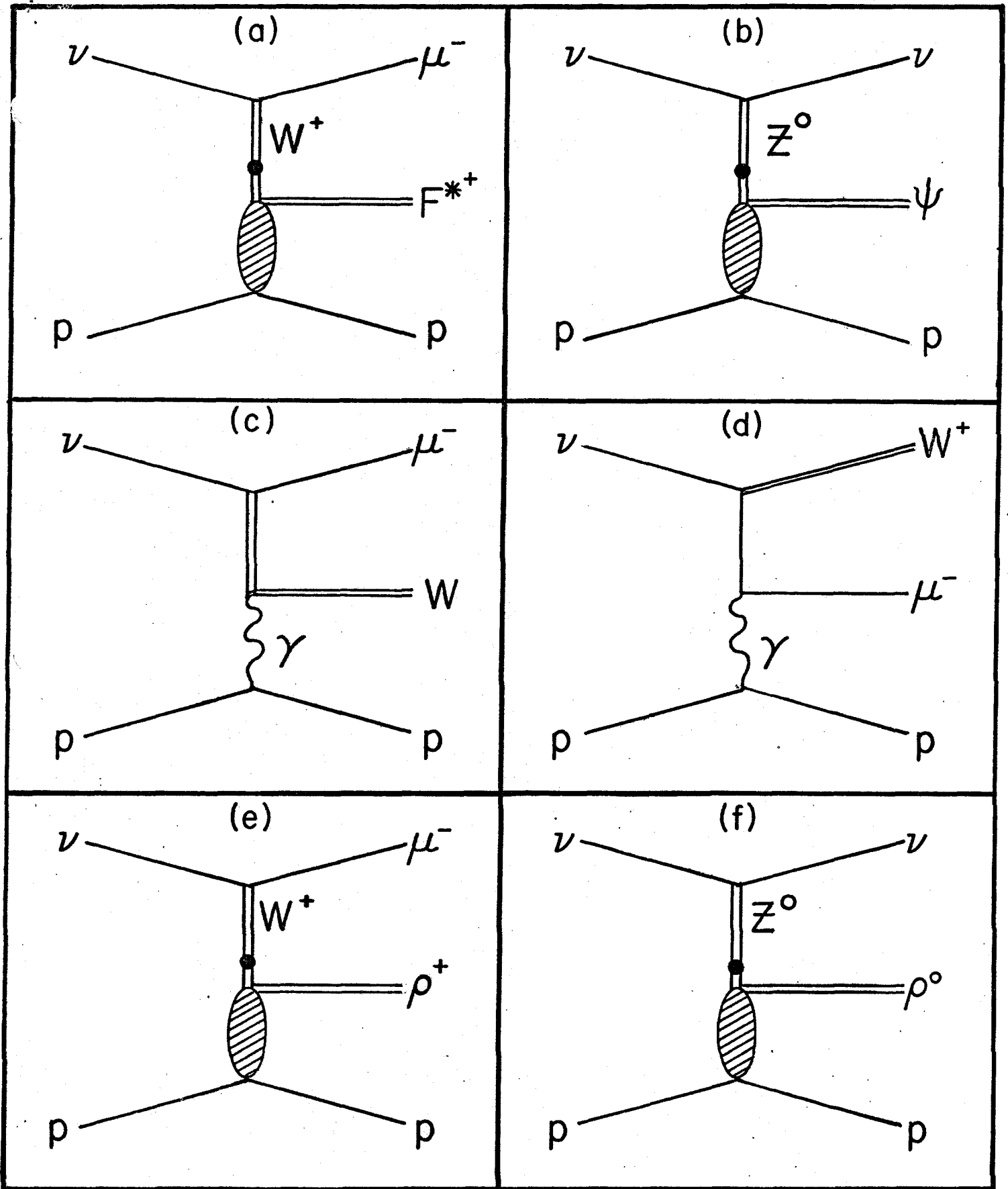


FIG. 3. Normalized probability distribution for electron energy loss via bremsstrahlung for  $t = 0.25$  radiation lengths.



THREE BODY DIAGRAM

FIG. 4.

## 15-FOOT BUBBLE CHAMBER WITH PLATES

S. J. Barish, R. Brock, A. Engler, T. Kikuchi, R. Kraemer,  
F. Messing, B. Stacey, M. Tabak  
Carnegie-Mellon University  
Pittsburg, Pennsylvania 15212

and

J. P. Berge, D. V. Bogert, R. Hanft, J. A. Malko, F. A. Nezrick  
W. Smart, and J. Wolfson  
Fermi National Accelerator Laboratory  
Batavia, Illinois 60510

and

R. J. Endorf  
University of Cincinnati  
Cincinnati, Ohio 45221

December 30, 1977

## ABSTRACT

We propose a study of broad-band neutrino interactions in the  $H_2$  filled 15-foot bubble chamber containing a Plate Converter System (PCS). The PCS system allows one to study interactions on free protons while simultaneously obtaining a 75% gamma ray conversion efficiency and 95% electron and muon identification. We request an exposure of  $6 \times 10^{18}$  protons on the target of the horn system at 400 GeV. Based on measured yields from E45 we expect 15,000 neutrino proton events in this exposure. The two main physics goals of the proposed experiment are a general study of charmed particle production mechanisms and a study of the neutrino-proton cross sections for neutral current and charged current interactions. The charmed particle investigation will include studies of both inclusive and exclusive production. Both of these studies are greatly aided by the PCS ability to detect final state gamma rays and electrons with high efficiency.

FERMILAB

JAN 4 1978

LIBRARY

## I. INTRODUCTION

We request a neutrino exposure in the H<sub>2</sub> filled 15-foot bubble chamber using a downstream Plate Converter System (PCS). The requested exposure is for  $6 \times 10^{18}$  protons at 400 GeV on the target of the horn focussing system. This exposure will produce about 15,000 events on free protons. Table I shows the distribution of events in specific final states. The main features of this experiment are the ability to study interactions off a free proton target and to simultaneously obtain a 75% gamma ray conversion efficiency and 95% electron and muon identification. Only a PCS or a track sensitive target (TST) system allows one to obtain both of the above features simultaneously. The PCS system, however, has the distinct advantage of a significantly increased fiducial volume (approximately a factor of 3) in comparison to any reasonable TST arrangement for the 15-foot chamber.

A discussion of the PCS system is presented in Section II. Appendix A gives the response to the Program Advisory Committees specific questions concerning the utility of plates in the 15-foot bubble chamber. A comparison of the PCS, TST, and H-Ne filling systems is presented in Table II.

The primary physics objective in this experiment described in Section III, are:

- (1) Measurement of the neutrino-proton differential cross sections for neutral and charged current interactions.
- (2) A search for charmed particle production and decay both leptonically and non-leptonically.
- (3) A study of dilepton production off free proton targets.
- (4) A study of exclusive reactions off free protons.
- (5) A search  $\nu_{\mu}$ -e elastic scattering.
- (6) A search for heavy lepton production.
- (7) A study of parton fragmentation.

## II. DESCRIPTION OF THE PCS SYSTEM

The PCS combines most of the best features of the hydrogen bubble chamber, the heavy liquid bubble chamber, and the track sensitive target (TST) while incorporating new features not found in any of these instruments. This PCS arrangement is the product of the September 16, 1977 Neutrino Department meeting on plate proposals for the 15-foot bubble chamber. The PCS system (Fig. 1) consists of four steel plates, 1/2 inch (0.7 radiation length) thick and separated by 25 cm at the chamber midplane. Each plate is tilted to present minimum obscuration to two cameras ( 2 and 3) while allowing an unobstructed view of the target fiducial volume by all cameras.

The proposed PCS configuration provides 2.9 radiation lengths of metal for conversion of forward photons. This results in

an average conversion probability of 70% for all photons produced within the fiducial volume. Due to the correlation between angle and energy, 79% of the energy which goes into photons will become visible using the PCS. A comparison with other systems is given in Table III.

Electrons from gamma rays converting in the plates are typically measured for only  $\sim 20$  cm in the PCS giving  $\Delta P/P \approx 2\%$  (20%) for  $P \sim 1$  GeV ( $\sim 10$  GeV/c). Using the Mo-Tsai approximation to estimate the electron multiple scattering in the plates gives  $\Delta P/P$  of  $\sim 0.39$  for one electron and  $\sim 0.31$  for a  $\gamma$ -ray. The corresponding  $\pi^0$  fractional momentum error is 0.17 before fitting.

Electrons from the neutrino interaction will be identified with efficiency  $> 95\%$  from bremsstrahlung in the plates or via their characteristic spirals for low energy. Muons of momentum greater than 4 GeV/c will be identified with efficiency  $> 95\%$  by a combination of the EMI and plate penetration.

The fiducial volume with the plate arrangement is  $15.7 \text{ m}^3$ ,  $13.7 \text{ m}^3$ , or  $11.5 \text{ m}^3$  according to whether the fiducial volume is terminated at the first plate, 30 cm upstream of the first plate, or 60 cm upstream of the first plate. The direct competition to the physics of these runs, the study of  $\nu$  and  $\bar{\nu}$  interactions off free neutrons and free protons will come from the CERN TST which will have a fiducial volume of about  $3 \text{ m}^3$ .

Since, for example in E45  $\sim 90\%$  of the hadrons have momenta less than 10 GeV, the fiducial volume is primarily limited by the length of track required to measure the muon. Muon tracks

can be measured through the plates. Even if the fiducial volume is terminated only 30 cm upstream of the first plate, the minimal muon track length would be 1.2 m. The track momentum error  $\Delta P/P$  as determined by a good geometry program are given in Table IV for various momenta and measured lengths.

The determination of the non-neutrino backgrounds in the chamber can best be done with a hydrogen fill in the chamber. One performs kinematic fits of  $H_2$  events to reactions such as  $np \rightarrow pp\pi^-$ ,  $K_L^0 p \rightarrow K_S^0 p$ ,  $K_L^0 p \rightarrow K^+ p\pi^-$ .

### III. PHYSICS

#### A. Exclusive Channels

A distinct advantage of the PCS in  $H_2$  is the ability to study exclusive reactions including those with a final state  $\pi^0$  using 3-constrained fits. High energy events in bare hydrogen experiments involving unseen gamma rays give false 3-constraint fits about 15% of the time. Using the PCS system the probability of false fits can be reduced to 3%.

Some exclusive reactions which are of particular interest are events containing neutral strange particles, meson resonances and baryon resonances. Reactions involving strange particles are important because they provide information on charm production, selection rules and further properties of the weak charged and neutral currents. From diffractive  $\rho$  production in charged and neutral current interactions one can learn about  $W^+ \rho^+$  and

$Z^0$ - $\rho^0$  coupling. For this study it is important to detect  $\pi^0$ 's. The study of two-body reactions involving the baryonic resonances  $\Delta^{++}$ ,  $\Delta^+$ ,  $N^+$  is also enhanced by use of the PCS system.

### B. Charm Particle Searches

The discovery of charmed particle production in  $e^+e^-$  experiments at SLAC has added new impetus to the search for these particles in neutrino induced interactions. These new particles and others as yet undetected can be expected to decay both leptonically and non-leptonically. The PCS gives one the possibility of detecting charmed decays in many different decay modes. Assuming an overall charm-particle rate of 5% of the charge current events, we can expect to have  $\sim 600$  charmed particle events in our data. We will search for charm production both inclusively and exclusively. For an inclusive study we can, for example, look for charm-signals in effective-mass distributions of various particle combinations. Of particular interest will be the effective mass distributions containing a  $\Sigma^+$ ,  $K^\pm$ ,  $K^0$  or  $\Lambda$ , since in the GIM scheme charmed particles are expected to decay frequently into strange particle final states.

By studying exclusive channels with exotic final states one might also see evidence for charm production. For example, the  $\nu p \rightarrow \mu^- \pi^+ \pi^+ \pi^-$ ,  $\Delta S = -\Delta Q$  event observed at BNL is thought to be an example of charm production. Here again, as in the general study of exclusive channels, the PCS ability to detect missing neutrals will help in obtaining a clean sample of 3-c fits.

### C. Study of Di-Lepton Production

The observation of neutrino-induced  $\mu^- \mu^+$  production and  $\mu^- e^+ K_S^0$  production in heavy nuclear targets has emphasized the importance of the weak interaction in new particle production. The proposed PCS experiment will provide an improved understanding of these phenomena. The detection of the  $\nu p \rightarrow \mu^- e^+ X$  channels will be greatly facilitated by an electron detection efficiency  $> 95\%$  at all momenta. The total background in the  $\mu^- e^+ X$  sample from asymmetric Dalitz pairs, close in gamma conversions, electrons from undetectable meson decays, etc., will be acceptably low. By taking advantage of the PCS ability to detect  $\pi^0$ 's one can use the zero-constraint fits assuming an undetected final state neutrino) to estimate the incident neutrino energy  $E$ ,  $W$  (total hadronic mass),  $q^2$ ,  $x$ , and  $y$ . In addition, other details of the hadronic vertex can be studied, such as the neutral multiplicity, and various effective mass combinations of the  $e^+$ ,  $\nu_e$  and hadrons.

### D. Deep Inelastic Scattering

Experiments on deep inelastic neutrino scattering produce fundamental information about the structure of the proton which cannot be obtained from electron and muon experiments. Many aspects of the existing data support a simple quark parton picture for the nucleons. However deviations from the predictions of scaling and evidence for new particle production based on scaling distributions have been reported in neutrino experiments.

1) Charged Current Reactions

From a combination of EMI data and plate penetration we can identify  $\sim 85\%$  of the charged current events. Since neutral pions will be detected, we expect  $\Delta E_H/E_H < 0.10$  from track measurements alone. Using a transverse momentum balance procedure we can reduce the error in  $E_\nu$  to  $\sim 2\%$ . Table IV shows a comparison of the resolution which can be obtained in bare  $H_2$  and PCS with  $H_2$ . The improved resolution in x and y will make it easier to detect and measure any "anomalies" in the scaling distributions. The resolution in W is about four times better than in the bare and the sensitivity of a search for narrow baryon states is greatly improved.

2) Neutral-Current Reactions

The space-time structure of the weak neutral-current is one of the most central questions in weak-interaction physics. By using the PCS in the 15-foot chamber, we propose to measure the inclusive distributions for neutral-current  $\nu p$  interactions, and hopefully determine the space-time structure of the neutral-current. The neutral- and charged-current events can be clearly separated using the PCS and the EMI.

Most reasonable models of weak neutral current contain coupling constants which determine the mixing of vector, axial-vector, isoscalar, and isovector components of the current. The most straightforward way of determining these constants is by measuring cross sections from free nucleon targets with free proton targets. In an experiment with free proton targets, the

constants can be determined by studying the differential cross sections.

The neutrino  $y$  (where  $y = E_{\text{hadron}}/E_{\text{neutrino}}$ ) distribution is

$$\frac{d\sigma}{dy}(\nu p) = g_R^P (1-y)^2 + g_L^P .$$

For a pure vector, isoscalar current the relation  $g_L^P = g_R^P$  holds while for the Weinberg-Salam model (with  $\sin^2 \theta_W = 0.23$ ),  $g_L^P = .92$ ,  $g_R^P = 0.05$ . One can measure distributions in the variable  $u = x(1-y) \approx P_H g_H^2 / 2M_p$  which depends only on the variables of the hadron system. Measurements of the charged hadron momentum with low multiple scattering and low interaction probability will provide a precision measurement of  $P_H(\text{charged})$ . The photon conversion plates will provide  $\sim 70\%$  of the remaining hadron momentum which would otherwise disappear in neutral mesons. With the neutral and charged components combined, we expect  $\Delta u \approx .01$ . With this resolution the unfolding of the coupling constants will be possible. Without the plates  $\Delta u \approx .05$ . To demonstrate the need for the resolution provided by the plates, we show the theoretical  $u$  distributions (Fig. 2) for several forms of the neutral current.

#### F. Pure Leptonic Interactions

The 4-Fermion reactions in the hydrogen of the type  $\nu_\mu e^- \rightarrow \mu^- \nu_e$  and  $\nu_\mu e^- \rightarrow \nu_\mu e^-$  should be detectable. Backgrounds from reactions on protons in which two positive charges are not detected

are negligible. Background to the second reaction from  $\nu_e e^- \rightarrow \nu_e e^-$  will be small since the  $\nu_e$  flux is 3 orders of magnitude smaller than the  $\nu_\mu$  flux.

G. Heavy Lepton Production

We intend to search for the production of charged heavy leptons which could decay by any of the following modes:

$L \rightarrow l \gamma; l + \text{hadrons}; l \bar{\nu}_e \nu_L; \nu_L + \text{hadrons}$ . Thus to detect and study heavy leptons one again needs good identification and measurement of gammas and charged leptons.

SUMMARY

This proposal using the PCS system allows a study of neutrino interactions on free protons while simultaneously having a 75% gamma conversion efficiency and a 95% efficiency to identify electrons and muons. These unique advantages of the PCS system make possible the study of charmed particle production mechanisms and a study of the neutrino proton differential cross sections for neutral current and charged current interactions.

TABLE I  
 YIELDS OF NEUTRINO EVENTS INSIDE  
 FIDUCIAL VOLUME FOR PCS  
 (based on E45 measurements)

Reaction	Number of Events <sup>*</sup>
$\nu_p \rightarrow \mu^- X$	12,000
$\nu_p \rightarrow \nu X$	3,000 <sup>†</sup>
$\nu_p \rightarrow \Lambda X$	600 <sup>‡</sup>
$\nu_p \rightarrow K_S^0 X$	600 <sup>‡</sup>
$\nu_p \rightarrow \mu^- e^+ X$	120
$\nu_p \rightarrow \mu^- \mu^+ X$	120
TOTAL $\nu_p$	15,000
$\nu_\mu e^- \rightarrow \mu^- \nu_e$	~ 40
$\nu_\mu e^- \rightarrow \nu_\mu e^-$	~ 50
TOTAL $\nu_\mu e$	~ 90

\* 400K pictures,  $1.5 \times 10^{13}$  ppp, 400 GeV/c protons, 2 horns, 12 m<sup>3</sup> fid. vol.,  $\Sigma P_x$  (vis.) > 9 GeV/c.

<sup>†</sup>  $\Sigma P_x$  (vis.) > 5 GeV/c for neutral current events.

<sup>‡</sup> charged (i.e., visible) decays only.

TABLE II

COMPARISON OF PCS, TST AND H-NE

Parameter	PCS	TST	H-Ne (atomic)	
			20%	100%
Ave. $\gamma$ detection efficiency	75%	90%	70%	99%
$\Delta P/P$ for $\pi^0$ (before fitting)	>20%	8%	6%	10%
H <sub>2</sub> fiducial volume (m <sup>3</sup> )	$\sim 12$	$\sim 3$	-	-
Ability to measure $\sigma(n)/\sigma(p)$	poor	good	poor	poor
Ability to study $V^0$ decays	exc.	exc.	exc.	good
Ability to study kink decays	exc.	exc.	poor	poor
$\mu$ detection efficiency (> 2 GeV)	>95%	>95%	>95%	> 95%
e detection efficiency (after measurement)	>95%	>95%	>95%	>97%

TABLE III  
RESOLUTION FOR THE BARE H<sub>2</sub> CHAMBER AND  
FOR PCS WITH H<sub>2</sub>

Variable	Charged current events	
	Bare H <sub>2</sub>	PCS + H <sub>2</sub>
E <sub>v</sub>	~ 8%	~ 2%
x	~ .03	~ .007
y	~ .04	~ .01
q <sup>2</sup>	~ 8%	~ 2%
v	~ 16%	~ 4%
W	~ 8%	~ 2%

Note: Numbers quoted as percentages are fractional resolutions and decimal numbers are absolute resolutions.

TABLE IV  
TRACK FRACTIONAL MOMENTUM ERROR AS A  
FUNCTION OF MEASURED LENGTH

Momentum (GeV/c)	Measured Length				
	0.3 m	0.6 m	1.0 m	2.0 m	3.0 m
1.0	4.0%	0.9%	0.4%	0.15%	-
2.5	9.0%	2.5%	0.8%	0.3%	0.1 %
5.0	20.0%	4.0%	1.5%	0.4%	0.15%
10.0	35.0%	9.0%	4.0%	0.8%	0.4%
50.0	-	-	16.0%	4.0%	1.0%

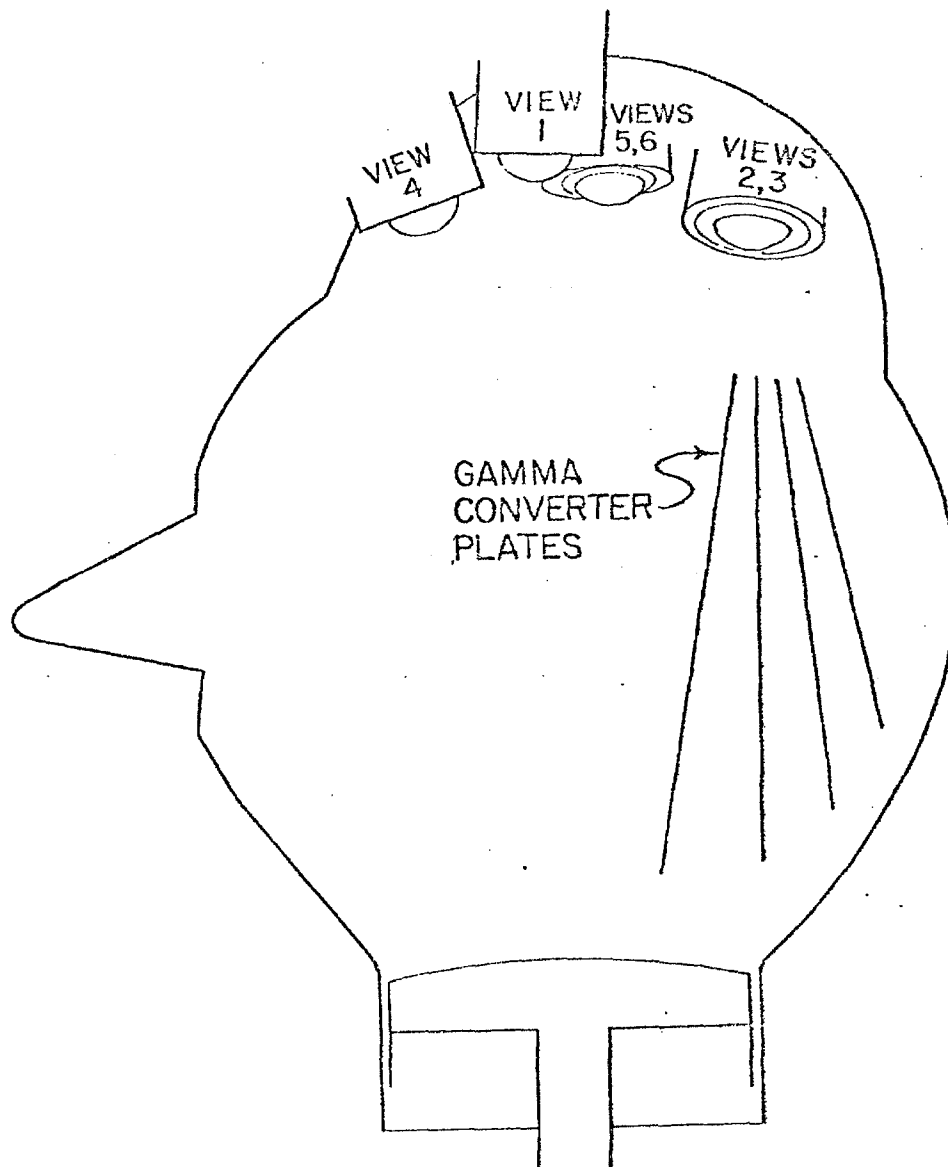


Figure 1

Pictorial representation of the 15-foot bubble chamber with gamma ray converter plates. The four plates are stainless steel, each one-half conversion length thick (~13 mm) and ~25 cm apart in the mid-plate.

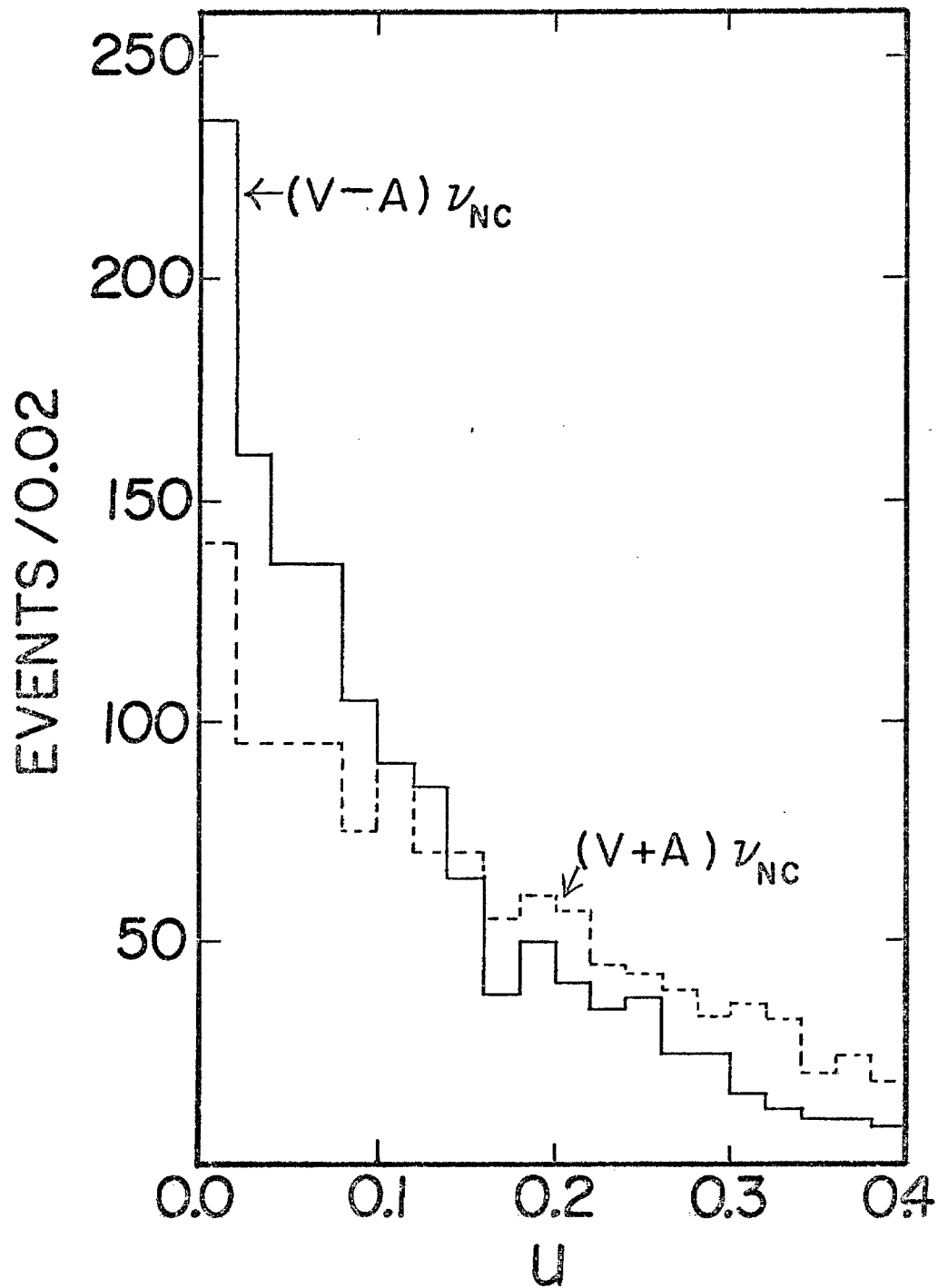


FIGURE 2

U distributions for Monte-Carlo generated neutrino neutral current events with V-A and V+A form for the interaction. The estimated measurement error is included.

## APPENDIX A

Response to PAC's questions concerning experiments using plates in the 15-foot bubble chamber (Presented by D. Duane Carmony).

### I. Turbulence and Distortion Due to Plates

#### Question:

There was a general concern about the precision with which gamma ray energies could be determined on the basis of measurements made on electron pairs between the plates. In the past, distortion of the tracks between the plates due to turbulence and fluid motion has been a problem with this procedure. The Committee suggested that you review the experience at Brookhaven and then revise your estimates if this seems necessary.

#### Reply:

Recent experience with measurements of tracks between plates has been obtained at BNL and SLAC. Conversations with N.P. Samios and M. Murtagh at BNL (by A. Engler) reveal that no measurable turbulence exists in the BNL 7-foot chamber. It should be pointed out that BNL has two inch thick plates with gaps of two inches between them - a system quite different from the one we are proposing. Their experience has been sufficiently encouraging that they are planning to build a thin plate system for the 7' chamber which would be suitable for  $\gamma$ -ray energy determination. C. Field from SLAC also reported no measurable turbulence for their arrangement of three plates each one radiation length thick with plate separations of 9 cm. Furthermore, Field reported that converted  $e^+e^-$  pairs of energy greater than 50 MeV point back to the production vertex. There is therefore every reason to expect determination of  $\gamma$ -ray energies as outlined in our proposals.

## II. Reconstruction of $\pi^0$

### Question:

You stated in your presentation that you had not attempted an estimate of how well  $\pi^0$ 's could be reconstructed. The Committee would appreciate a quantitative estimate of this if it can be arrived at in a reasonable length of time.

### Reply:

We have obtained an estimate for  $\pi^0$  mass reconstruction from converted  $e^+e^-$  pairs using a Monte Carlo simulation based on the assumption that the  $\pi^0$  momentum and multiplicity distributions are equal to the  $\pi^-$  distributions observed in E-31. Photons resulting from the  $\pi^0$  decays were converted in the plates and the invariant mass was calculated from all possible photon pairs. We used our predicted uncertainty in  $\gamma$ -ray energies of about 30% and included measuring error uncertainties for the electrons. Using this simulation, the  $\gamma\gamma$  effective mass is shown for all  $\gamma\gamma$  combinations in Fig. II-1a and for the correct  $\gamma\gamma$  pairings in Fig. II-1b. The signal to noise ratio when all  $\gamma\gamma$  combinations are made is about 1:1 where the noise comes from wrong pairings. The correct combinations reproduce the  $\pi^0$  peak with a FWHM of  $\sim 80$  MeV. If we restrict ourselves to those events with two converted gammas (Fig. II-2), we note that they are primarily from single  $\pi^0$  events and that much of the multi-neutral pion background (shown shaded) can be removed by a suitable mass cut. The above estimates are derived solely from the direction and energy of the converted  $\gamma$ -rays. We expect to be able to improve on this by using the kinematics of the production vertex.

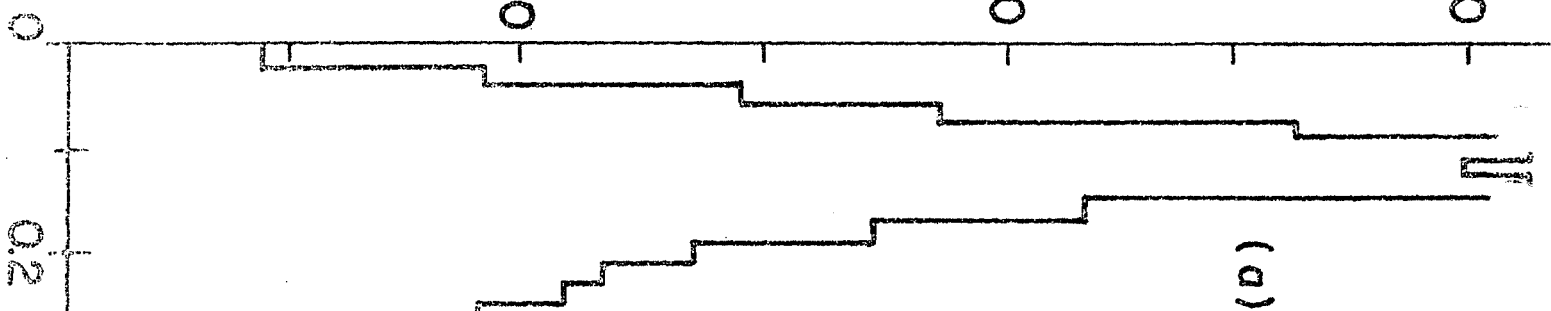
It should be emphasized that reconstruction of the individual  $\pi^0$ 's is only one objective. As has been pointed out, several perhaps more important reasons for adding the plates are: a) They greatly improve the measurement of hadronic energy and momentum for each event. The plates make possible a better measured angular distribution  $d^2\sigma/dx dy$  of free protons and neutrons for the charged current events. We experience no difficulty (due to secondary interactions close to the vertex) in reconstructing high  $y$  (that is, generally larger multiplicity) events in the light liquid. In the case of neutral currents the form of the interaction can be studied in terms of the scaling variable  $u = x(1-y) \approx P_H^2/2M_P$  which is well measured. b) The absence of  $\gamma$ -rays in the plates is an indicator of potential  $3c$  candidates involving no  $\pi^0$ 's. Used as a veto in selecting  $3c$  candidates the plates improve the signal to noise from 1:15 to about 3:1. Much of the remaining background can be removed by the kinematic fitting since the missing gammas preferentially carry away considerable transverse momentum. c) The plates serve as an identifier of directly produced electrons. Thus both hadronic and semileptonic decays of charmed particles can be studied in these exposures.

Events Per 0.02 GeV

100

200

300



Events Per 0.02 GeV

50

100

150



Myr (GeV)

Myr (GeV)

FIG. III

0 0.2 0.4 0.6 0.8 1.0 1.2 1.4 1.6

0 0.2 0.4 0.6

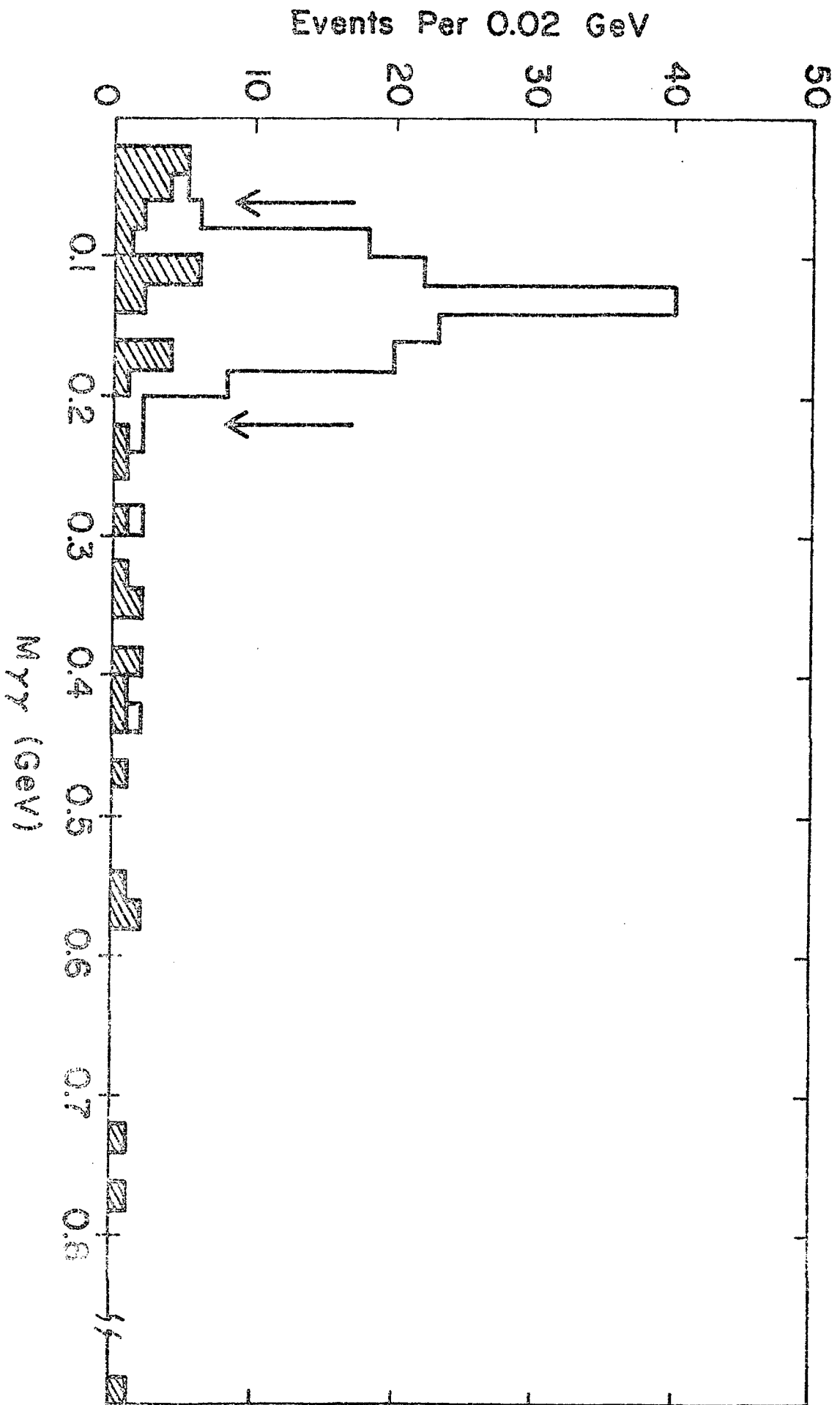


FIG. 11-2

### III. Fiducial Volume

#### Question:

Some members of the Committee felt that insufficient volume has been assumed to provide track measurements over sufficient length to achieve the charged track measurement errors you claimed (a few percent). If this turns out to be the case it could mean that the effective fiducial volume would end up substantially less than that assumed in the proposals. The Committee recommended that you reexamine this matter.

#### Reply:

The fiducial volume used by E-45 is about  $17\text{m}^3$  and allows 65cm downstream of the fiducial volume for secondary track measurements. The fiducial volume used by E-31 is  $18.7\text{m}^3$  and allows 25cm between the end of the fiducial volume and the chamber wall. The difference in volume is in part justified by the fact that the average energy of the events in E-31 is lower.

The fiducial volume with the plate arrangement which was presented at the previous PAC meeting is  $15.7\text{m}^3$ ,  $13.7\text{m}^3$ , or  $11.5\text{m}^3$  according to whether the fiducial volume is terminated at the first plate, one foot (30cm) back from the first plate, or two feet (60cm) back from the first plate. The direct competition to the physics of these runs, the study of  $\nu$  and  $\bar{\nu}$  interactions off free neutrons and free protons, will come from the CERN TST which will have a fiducial volume of about  $3\text{m}^3$ .

There is no one fiducial volume common to all the physics objectives. Dilepton ( $\mu e$ ) candidates which occur just upstream or even between the plates will be studied.

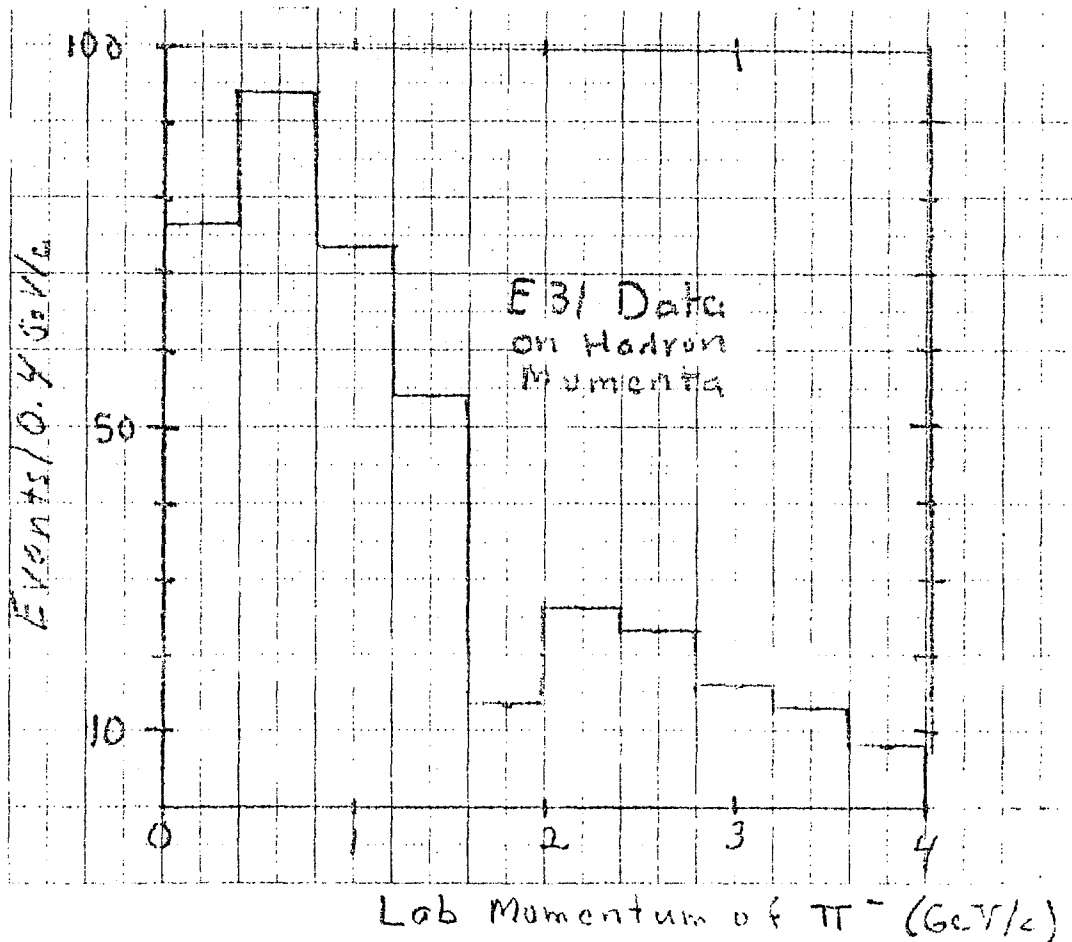
We further remark that, since for example in E-31 98% of the hadrons have momenta less than 10 GeV, the fiducial volume is primarily limited by the length of track required to measure the muon. Muon tracks can be measured through the plates. Even if the fiducial volume is terminated only one foot

upstream of the first plate, the minimal muon track length would be 1.2m instead of the 0.3 to 0.65m currently used by E-31 and E-45.

The error  $\Delta p/p$  in per cent as determined by a well tuned TVGP (such that chi squared probability distributions from subsequent fitting are reasonably flat) are tabulated for various momenta (GeV/c) and Lengths (meters) below:

Table of  $\Delta p/p(\%)$

Momentum (GeV/c)	Length $\rightarrow$				
	0.3m	0.6m	1.0m	2.0m	3.0m
1.0	4.5%	1.3%	0.5%	0.4%	---
2.5	13%	3.2%	1.4%	0.3%	0.2%
5.0	20%	6%	4%	0.9%	0.3%
10.0	65%	12%	6%	1.8%	0.6%
50.0	---	---	42%	11%	3%



#### IV. Neutral Currents

##### Question:

The study of neutral currents is one of the main thrusts of a number of the plates proposals. The Committee has requested that you provide the best quantitative estimates you can of how effective these experiments would be in investigating those phenomena. In particular, studies of neutral current phenomena in the 15-ft bubble chamber with the broad band beam in the past have had a difficult time with charged current backgrounds. How serious would that be in the new proposed experiments with plates? What are the most convincing arguments you can make that you can even do the neutral current studies with the broad band beam? How would you expect the results obtained with plates to compare with those expected from the experiments utilizing the dichromatic beam with a neon mixture in the bubble chamber?

##### Reply:

Any attempt to study the details of the neutral current interaction in the 15-foot bubble chamber requires the improved EMI. This statement is independent of the liquid, the beam or the plate arrangement used. One expects the EMI to achieve a muon detection efficiency of  $\sim 95\%$  with quite low hadron punch through. Nearly all the charged current background will be removed using the EMI. In addition, the improved determination of  $E_H$  and  $\vec{P}_H$  which the plates provide improves the "kinematic algorithm" (non-EMI) for selecting muon candidates.

Most reasonable models of weak neutral current contain four coupling constants which determine the mixing of vector, axial-vector, isoscalar, and iso-vector components of the current. The most straightforward way of determining these constants is by measuring cross sections from proton and neutron targets separately. This requires the use of  $H_2/D_2$  fills since secondary interactions in heavy target nuclei introduce severe systematic uncertainties which prohibit clean neutron-proton separation. Using isoscalar targets permits measurement of only two relationships among the four coupling constants. In an experiment with free nucleon targets, all four constants can be determined simultaneously by studying the differential cross sections. This can be seen for example in

the antineutrino  $y (= E_{\text{hadron}}/E_{\text{neutrino}})$  distributions:

$$\frac{d\sigma}{dy} (\nu P) = g_L^P (1-y)^2 + g_R^P$$

$$\frac{d\sigma}{dy} (\nu N) = g_L^N (1-y)^2 + g_R^N .$$

For a pure vector, isoscalar current the relation  $g_L^P = g_R^P = g_L^N = g_R^N$  holds while for the Weinberg-Salam model (with  $\sin^2 \theta_w = .23$ )  $g_L^P = .92$ ,  $g_R^P = .05$ ,  $g_L^N = .48$ ,  $g_R^N = .04$ . One can measure distributions in the variable  $u = x(1-y) = P_H \theta_H^2 / 2M_P$  which depends only on the variables of the hadron system. Measurements of the charged hadron momentum with low multiple scattering and low interaction probability will provide a precision measurement of  $\vec{P}_H$  (charged). Photon conversion plates will provide  $\sim 70\%$  of the remaining hadron momentum which would otherwise disappear in neutral mesons. With the neutral and charged components combined, we expect  $\delta u \sim .01$ . With this resolution the unfolding of the coupling constants will be possible. Without the plates  $\delta u \sim .05$ . To demonstrate the need for the resolution provided by the plates, we show the theoretical  $u$  distributions (Fig. IV-1) for several forms of the neutral current.

It should also be noted that in the case of a  $D_2$  fill, the neutron and proton targets are exposed to precisely the same flux spectrum so that these results will not depend on normalizations or on spectrum calculations as in the case of  $\nu$ ,  $\bar{\nu}$  cross section comparisons.

In a narrow band beam the NC/CC separation is easier when the outgoing neutrino has a large fraction of the energy. For large  $y$ , however, the outgoing neutrino is soft and these experiments will need the EMI for charged current identification. In heavy Neon, about 10% of the events are unmeasurable and these tend to be the high multiplicity i.e., large  $y$ -events. The narrow band experiments proposed all have events at much higher energy than the average

energy of broad band events. This makes the experiments complementary.

In summary, it should be possible to do rather detailed measurements in the light liquid + plates experiments. These measurements of free protons and neutrons cannot be achieved by heavy liquid bubble chambers or counters.

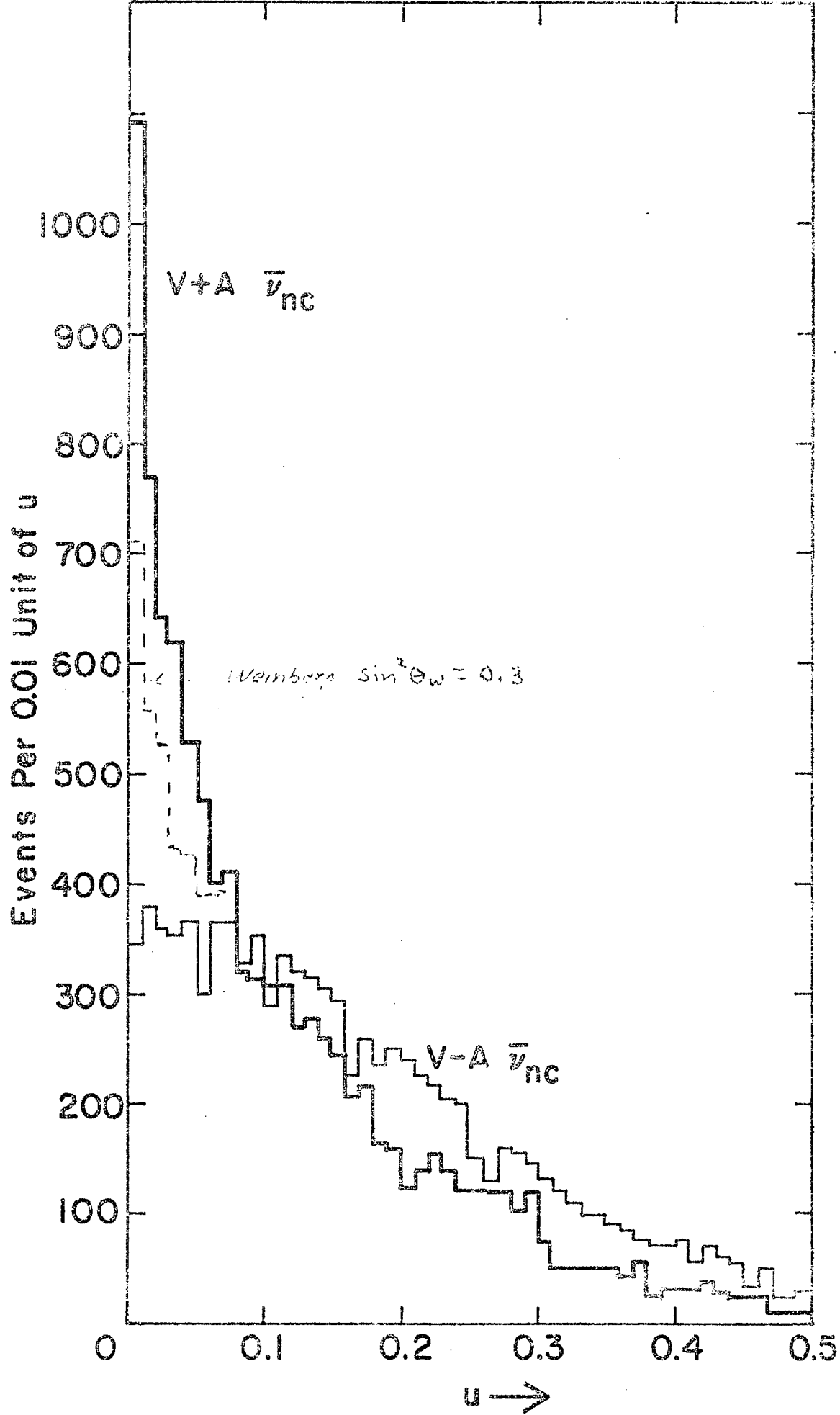


Fig. IV-1

## 7. Electron Identification

### Question:

The Committee felt that the very good rejection of pions you claimed could be attained with the plate system utilized as an electron identifier, seemed contrary to past experience. They suggested that you study experimental results obtained elsewhere and furnish a more detailed explanation of why you think the plates would be so much more effective.

### Reply:

We believe that the claims for electron identification as stated at the October PAC are consistent with results at other laboratories. The most detailed work has been done at SLAC and is reported on more fully in the appendix to this section. This report can be summarized:

The plate system used at SLAC (three tantalum plates each one radiation length thick with 9 cm plate separation) has approximately the same  $e^\pm$  detection properties as the proposed plate system for the Fermilab 15-foot bubble chamber. The conclusions of the BC-65 collaboration (Duke, SLAC, and Imperial College) are based on electron and pion calibration runs at 1.6 and 3 GeV/c. They concluded (a) at 1.6 GeV/c, approximately one incident  $\pi^\pm$  in 20,000 causes a fake  $e^\pm$  shower, and (b) at 3.1 GeV/c, approximately one incident  $\pi^\pm$  in 100,000 causes a fake  $e^\pm$  shower, and (c) a good signature for true  $e^\pm$  tracks occurs  $(94 \pm 1)\%$  of the time above 1 GeV/c.

We believe that our discrimination against hadrons could be as much as three times poorer than the above numbers because we are using steel plates. These calibration results are in the proper momentum range for dilepton events. Because of the falling charge exchange cross section, the rejection of pions at higher energies is expected to be even better.

We also note that Kitagaki et al., submitted a paper<sup>22</sup> to Hamburg on "Direct Electron Production in 8 GeV/c  $\pi^-p$  and 15 GeV/c  $\bar{p}p$  Interactions." They utilized

---

<sup>22</sup>T. Kitagaki, S. Tanaka, H. Yuta, K. Abe, K. Hasegawa, A. Yamaguchi, T. Nozaki, K. Tamai, R. Kikuchi, T. Maruyama, Y. Unno, S. Kunori and Y. Ohotani (Tohoku University preprint TUHEL 77-4).

the BNL 30" chamber with two tantalum plates each 1.6 radiation lengths thick and separated by 14cm. They successfully measured direct  $e/\pi$  production ratios of  $1.8 \pm 1.1 \times 10^{-4}$  and  $< 4.7 \pm 2.8 \times 10^{-4}$  for  $\pi^-$  and  $\bar{p}$  respectively.

Scientific Spokesman: Frank A. Nezrick  
Fermi National Accelerator Laboratory  
P. O. Box 500  
Batavia, Illinois 60510

STUDY OF NEUTRINO INTERACTIONS IN HYDROGEN USING THE 15-FT.  
BUBBLE CHAMBER AND ITC SYSTEM

S. J. Barish, A. Engler, G. Keyes, T. Kikuchi,  
R. Kraemer, and B. Stacey  
Carnegie-Mellon University  
Pittsburg, Pennsylvania 15212

and

J. P. Berge, F. A. DiBianca, R. Hanft, J. A. Malko,  
F. A. Nezrick, W. G. Scott and W. Smart  
Fermi National Accelerator Laboratory  
Batavia, Illinois 60510

and

R. J. Endorf  
University of Cincinnati  
Cincinnati, Ohio 45221

March 25, 1977

## ABSTRACT

We propose a study of broad-band neutrino interactions in the H<sub>2</sub> filled 15-Ft. bubble chamber containing an Internal Target Converter (ITC) system. The ITC system allows one to study interactions on free protons while simultaneously obtaining a 90%  $\gamma$  conversion efficiency and 95% electron and muon identification. We request an exposure of  $4 \times 10^{18}$  protons on the target of the two-horn system at 400 GeV. Based on measured yields from E-45 we expect 15,000 neutrino proton events in this exposure. The two main physics goals of the proposed experiment are a general study of charmed particle production mechanisms and a study of the neutron to proton cross section ratio for neutral current and charged current events. The charmed particle investigation will include studies of both inclusive and exclusive production. Both of these studies are greatly aided by the ITC's ability to detect final state  $\gamma$ 's and electrons with high efficiency. Furthermore, the presence of nuclear targets will allow a comparison of dilepton production on protons and neutrons separately without the difficulty of having to know the incident neutrino flux.

## PREAMBLE

To illustrate the ITC technique we have used in this proposal a specific ITC arrangement of nine thin plates, which we feel is a reasonable first estimate of a possible ITC system. However, it is understood that if the research program for the 15-Ft. bubble chamber is approved using the ITC technique the relevant groups would work together to design a mutually acceptable ITC system.

## I. INTRODUCTION

We request a neutrino exposure in the H<sub>2</sub> filled 15-Ft. bubble chamber using an Internal Target Converter (ITC) system. The requested exposure is for  $4 \times 10^{18}$  protons at 400 GeV on the target of the two-horn focussing system. This exposure will produce about 15,000 events on free protons. Table I shows the distribution of events in specific final states. The main features of this experiment are the ability to study interactions off a free proton target and the ability to simultaneously obtain a 90%  $\gamma$  conversion efficiency and 95% electron and muon identification. Only an ITC or TST\* system allows one to obtain both of the above features simultaneously. The ITC system, however, has the distinct advantage of a significantly increased fiducial volume (approximately a factor of 3) in comparison to any reasonable TST arrangement for the 15-Ft. chamber.

A detailed discussion of the ITC system is presented in Section II and Appendix A of this proposal; a comparison of the ITC with downstream plates, TST, and H-Ne filling systems is presented in Appendix B with a  $\gamma$  conversion comparison in Fig. 1.

The primary physics objectives in this experiment, described in Section III, are: a study of exclusive reactions off free protons; a study of dilepton production off both proton and neutron targets; a measurement of the neutron and proton cross section

---

\*Fermilab Proposal 44A

ratio for neutral current and charged current events; a search for charmed particle production and decay both leptonically and non-leptonically; a study of deep inelastic scattering in charged current and neutral current events off proton and neutron targets separately; a search for  $\nu_e$  elastic scattering events, and a search for heavy lepton production.

## II. DESCRIPTION OF THE ITC SYSTEM

The ITC combines most of the best features of the hydrogen bubble chamber, the heavy liquid bubble chamber and the track sensitive target while incorporating new features not found in any of these instruments. In its general form an ITC consists of a series of thin high-Z plates dispersed through the fiducial volume of the chamber. The ITC system discussed here consists of nine thin steel plates, each 0.5 radiation lengths thick, and 30 cm apart at the chamber midplane with areas encompassing the usual fiducial volume. Each plate is tilted to present minimum obscuration to two cameras (#5 and #6) while allowing partial visibility of each track segment in a third view (#1). The appearance of the chamber with the proposed ITC configuration is shown in figures 2(a) and (b).

The general features of the ITC system are now discussed and further details are given in Appendix A.

### A. High Efficiency $\gamma$ Conversion

The proposed ITC configuration provides 4.5 radiation lengths of metal plus 0.3 radiation lengths of hydrogen. The average

$\gamma$  conversion efficiency for events distributed uniformly throughout the fiducial volume is 90% for a  $16 \text{ m}^3$  fiducial volume upstream of plate number 8. The  $\gamma$  conversion efficiency versus angle with respect to the  $\gamma$  direction is shown in Fig. 1 for ITC, TST, a downstream plate array, pure Ne, 20% atomic Ne and pure  $\text{H}_2$ . The ITC system fares very well in this comparison.

We now consider the resolution expected for  $\gamma$  momentum from the ITC. Electrons, typically measurable for only  $\sim 30 \text{ cm}$  in the ITC, will have  $\Delta p/p \sim 1\%$  ( $\sim 10\%$ ) for  $p \sim 1 \text{ GeV}/c$  ( $\sim 10 \text{ GeV}/c$ ).

Since converted electrons see, on the average,  $1/4$  radiation lengths of steel before reaching the hydrogen it is important to consider electron straggling (via bremsstrahlung) in the conversion plate. Figure 3 shows  $\phi(\alpha, t)$ , the probability that an electron retains a fraction  $\alpha$  of its incident energy after traversing  $t$  radiation lengths of steel. Using the Mo-Tsai<sup>1</sup> approximation for  $t = 0.25$ ,  $\bar{\alpha} = 0.75$ , and  $\delta\alpha(\text{r.m.s.}) = 0.29$ ,  $\Delta p/p$  is 0.39 for one electron and  $\sim 0.31$  for a  $\gamma$ . The corresponding  $\pi^0$  fractional momentum error is 0.17 before fitting.

#### B. Identification of Charged Leptons

Electrons of arbitrary momenta will be identified after measurement with efficiency  $> 95\%$  from bremsstrahlung in the plates or via their characteristic spirals for low energies.

Muons of momentum greater than  $4 \text{ GeV}/c$  will be identified with efficiency  $> 95\%$  by a combination of the EMI, and plate penetration. The plates will be most helpful in the angular region of  $60^\circ - 180^\circ$  where the EMI geometrical coverage is poor.

C. Momentum Resolution of Charged Hadrons

Since all tracks are detected and measured in hydrogen, the track reconstruction parameters are optimal. There are, however, two effects of the plates which must be considered: track length reduction from strong interactions and momentum resolution deterioration from multiple scattering.

The mean free path for hadrons (2 GeV/c pions) is 2.4 m in the proposed ITC configuration. The hadron interaction probability per plate is only 0.07. Thus, hadrons with momenta of several tens of GeV/c of which there are very few will typically have  $\Delta p/p < 2\%$ .

A typical (2 meter) track passes through 2.8 radiation lengths of converter and 0.2 radiation lengths of  $H_2$ . Then, as long as  $\beta \approx 1$ ,  $\Delta p/p$  from multiple scattering is  $< 2\%$ .

D. Simultaneous Studies of Neutrino Interactions on Free Nucleons and Heavy Nuclei

The ITC system provides the capability to study simultaneously interactions on both free protons and heavy nuclei (contained in the converting plates). Since the two types of targets are spatially separate, in contrast to H-Ne fills in which they are mixed, it is easy to identify the target in every event. The presence of nuclear targets will allow flux independent comparison of proton and neutron interactions.

E. Hydrogen Fiducial Volume

The hydrogen fiducial volume in the proposed ITC system is  $16 \text{ m}^3$  which is only slightly less than for a bare chamber (i.e.,  $20 \text{ m}^3$ ). It is difficult to design a TST for the 15-Ft. chamber with a hydrogen fiducial volume of much more than  $5 \text{ m}^3$ .

F. Measurement of Backgrounds

The non-neutrino backgrounds in the chamber can only be measured accurately with a hydrogen or deuterium fill in the chamber. One performs kinematic fits of  $\text{H}_2$  events to reactions such as  $n p \rightarrow p p \pi^-$ ,  $K_L^0 p \rightarrow K^0 p$ ,  $K_L^0 p \rightarrow K^+ p \pi^-$ . These fits can then be checked by observing the attenuation versus number of plates passed. In the  $\nu p$  bare chamber experiment,<sup>2</sup> these backgrounds were  $N_n / N_\nu^{\text{CC}} = (1.4 \pm 1.0)\%$  and  $N_{K_L^0} / N_\nu^{\text{CC}} = (1.2 \pm 1.2)\%$ .

G. Independence of Collision Length and Radiation Length

In H-Ne mixes and the TST arrangements one cannot specify the collision length and the radiation length independently because there is only one free parameter, the percent of Ne. However, with the ITC there are two independent variables, the atomic number and thickness of the plates. Thus one can first select the effective number of radiation lengths for the chamber and then choose the hadronic mean free path within a factor of 30 (C to Pb).

### III. PHYSICS

#### A. Exclusive Channels

A distinct advantage of the ITC in  $H_2$  is the ability to study exclusive reactions including those with a final state  $\pi^0$  using 3-constrained fits. High energy events in bare hydrogen experiments involving unseen  $\pi^0$ 's and  $\gamma$ 's give false 3-constraint fits about 15% of the time. Using the ITC system most of those false fits can be rejected.

Some exclusive reactions which are of particular interest are events containing neutral strange particles, meson resonances and baryon resonances. Reactions involving strange particles are important because they provide information on charm production, selection rules and further properties of the weak charged and neutral currents. Of special interest is the further pursuit of  $\Delta S = -\Delta Q$  reactions. A meson resonance of interest is diffractive  $\rho$  production in charged and neutral current interactions. From these events one can learn about  $W^+-\rho^+$  and  $Z^0-\rho^0$  coupling. For this study it is important to detect  $\pi^0$ 's. The study of two-body reactions involving the baryonic resonances  $\Delta^{++}$ ,  $\Delta^+$ ,  $N^+$  are also enhanced by use of the ITC system.

#### B. Charm Particle Searches

The discovery of charmed particle production in  $e^+e^-$  experiments at SLAC has added new impetus to the search for these particles in neutrino induced interactions.<sup>3</sup> These new particles and others as yet undetected can be expected to decay both leptonically and non-leptonically. Since the ITC can detect every type of stable particle except an outgoing neutrino, it gives

one the possibility of detecting charmed decays in many different decay modes. Assuming an overall charm-particle rate of 5% of the charge current events, we can expect to have ~ 600 charmed particle events in our data. If some of these charmed particles have only a few dominant decay modes, then we anticipate seeing signals from these decays. We will search for charm production both inclusively and exclusively. For an inclusive study we can, for example, look for charm-signals in effective-mass distributions of various particle combinations. Of particular interest will be the effective mass distributions containing a  $\Sigma^+$ ,  $K^{\pm}$ ,  $K^0$  or  $\Lambda$ , since in the GIM scheme charmed particles are expected to decay frequently into strange particle final states.

By studying exclusive channels with exotic final states one might also see evidence for charm production. For example, the  $\nu p \rightarrow \mu^- \pi^+ \pi^+ \pi^- \Lambda$ ,  $\Delta S = -\Delta Q$  event observed at BNL<sup>4</sup> is thought to be an example of charm production. Here again, as in the general study of exclusive channels, the ITC's ability to detect missing neutrals will help in obtaining a clean sample of 3-c fits.

### C. Study of Di-Lepton Production

The observation of neutrino-induced  $\mu^- \mu^+$  production and  $\mu^- e^+$  production in heavy nuclear targets has emphasized the importance of the weak interaction in new particle production. The proposed ITC experiment could provide a decisive understanding of these phenomena. The detection of the  $\nu p \rightarrow \mu^- e^+ X$  and  $\nu \text{Nuc} \rightarrow \mu^- e^+ X$  channels will be greatly facilitated by an electron detection efficiency  $> 95\%$  at all momenta. The total background in the  $\mu^- e^+ X$  sample from asymmetric Dalitz pairs, close-in  $\gamma$ 's, electrons from undetectable meson decays, etc., will

be acceptable. By taking advantage of the ITC's ability to detect  $\pi^0$ 's one can use the zero-constant fits (assuming an undetected final state neutrino) to estimate the incident neutrino energy  $E$ ,  $W$  (total hadronic mass),  $q^2$ ,  $X$ , and  $Y$ . In addition, other details of the hadronic vertex can be studied, such as the neutral multiplicity, and various effective mass combinations of the  $e^+$ ,  $\nu_e$  and hadrons. By taking advantage of the interactions in the steel plates we will also be able to make comparisons of  $\mu^-e^+$  and  $\mu\mu$  production off of neutron and proton targets.

#### D. Deep Inelastic Scattering

Experiments on deep inelastic neutrino scattering produce fundamental information about the structure of the neutron and parton which cannot be obtained from electron and muon experiments. Many aspects of the existing data support a simple quark-parton picture for the nucleons. Deviations from the predictions of scaling and evidence for new particle production based on scaling distributions have been reported in neutrino experiments.

##### 1) Charged Current Reactions

From a combination of EMI data and plate penetration we can identify 96% of the charged current events. Since neutral  $\pi^0$ 's will be detected, we expect a hadron energy determination which is considerably better than that for the bare chamber. One can measure  $W$ ,  $q^2$ ,  $\nu$ ,  $x$ ,  $y$  better than in a bare  $H_2$  chamber.

Table II shows a comparison of the resolution which can be obtained in bare  $H_2$  and ITC with  $H_2$ . The improved resolution in  $x$  and  $y$  will make it easier to detect and measure any anomalies in the scaling distributions. The resolution in  $W$  is about four times better and the sensitivity of a search for narrow baryon states is greatly improved.

Deep inelastic studies can be made on protons and nuclei simultaneously. This makes it possible to separate effects in the distributions ( $q^2$ ,  $\nu$ ,  $x$ ,  $y$ , etc.) which originate either with the proton or neutron target. Data on inclusive hadron production in charged current neutrino reactions are available from the bare chamber  $H_2$  experiment, but more precise results will be obtained with the ITC because the cc-nc separation is cleaner and  $E_\nu$  is better determined.

## 2. Neutral-Current Reactions

The space-time structure of the weak neutral-current is one of the most central questions in weak-interaction physics. The only real information on neutral-currents from the bare-chamber neutrino experiments has been measurements of the neutral-to-charged-current cross section ratios  $R_\nu$  and  $R_{\bar{\nu}}$ . Unfortunately, these measurements are not precise enough to impose constraints on the Weinberg-Salam model. By using an ITC in the 15-Ft. chamber, we propose to measure the inclusive  $x$  and  $y$  distributions for neutral-current  $\nu p$  interactions, and hopefully determine the space-time structure of the neutral-current. The neutral- and charged-current events can be clearly

separated using the ITC and the EMI. Since a large fraction of the  $\pi^0$ 's will be detected, it may be possible to make meaningful 0-c fits to determine the neutrino energy  $E_\nu$ ,  $x$ ,  $y$ ,  $q^2$ , etc. Table II shows the expected resolution for these variables from a Monte Carlo study.

E. Measurement of  $\sigma(n)/\sigma(p)$  for Charged and Neutral Currents

From measurements of relative production rates for charged and neutral currents on two types of targets containing different and known ratios of protons and neutrons, one determines  $\sigma(n)/\sigma(p) = \eta$ .

The ITC system with hydrogen is especially well suited to measure  $\eta_{cc}$  and  $\eta_{nc}$ . This is because the target (p or nucleus) is always identified since the targets are spatially separated and a statistical subtraction can be made. In  $D_2$  there is an uncertainty of  $\sim 10\%$  as to whether a proton or neutron was struck. In H-Ne mixes the uncertainty is much higher.

Both the absolute flux and the radial flux distributions cancel in ITC determinations of  $\eta_{nc}$  and  $\eta_{cc}$ . The errors in  $\eta_{cc}$  and  $\eta_{nc}$  come from the statistical error in the number of p events and from the cc/nc separation. Folding these together, we expect errors to be  $\sim 5\%$  for both  $\eta_{cc}$  and  $\eta_{nc}$  neglecting contributions from channels hard to detect and identify like  $\nu n \rightarrow \nu n$ .

At present  $\eta_{cc}$  is known to about 15% at low energy<sup>6</sup> and  $\eta_{nc}$  is unknown. Finally, we note that there is a simple relation between  $\eta_{cc}$ ,  $\eta_{nc}$  and the nc to cc ratios  $R_n$  and  $R_p$ , namely  $\eta_{nc}/\eta_{cc} = R_n/R_p$ .

#### F. Pure Leptonic Interactions

The 4-Fermion reactions in the hydrogen of the type  $\nu_{\mu} e^{-} \rightarrow \mu^{-} \nu_e$  and  $\nu_{\mu} e^{-} \rightarrow \nu_{\mu} e^{-}$  should be detectable. Backgrounds from reactions on protons in which two positive charges are not detected are negligible. Background to the second reaction from  $\nu_e e^{-} \rightarrow \nu_e e^{-}$  will be small (since the  $\nu_e$  flux is 3 orders of magnitude smaller than the  $\nu_{\mu}$  flux) unless this cross section is anomalously large. There is no way to separate these reactions.

The advantages of the ITC are (i) single negative prongs originating in the liquid will usually be identifiable in View #1 alone, (ii)  $\mu^{-}$  can be discriminated from  $e^{-}$  on the scan table by electron bremsstrahlung, (iii) possible additional  $\pi^0$  production can be vetoed on the scan table or after reconstructing any  $\gamma$ 's.

#### G. Heavy Lepton Production

We intend to search for the production of charged heavy leptons which could decay by any of the following modes:  $L \rightarrow \ell \gamma$ ;  $\ell + \text{hadrons}$ ;  $\ell \bar{\nu}_e \nu_L$ ;  $\nu_L + \text{hadrons}$ . Thus to detect and study heavy leptons one again needs good identification and measurement of gammas and charged leptons.

SUMMARY

This proposal using an ITC system allows a study of neutrino interactions on free protons while simultaneously having a 90%  $\gamma$  conversion efficiency and a 95% efficiency to identify electrons and muons. These unique advantages of the ITC system make possible the study of charmed particle production mechanisms and a study of the neutron to proton cross section ratio for neutral current and charged current events.

REFERENCES

- <sup>1</sup>Mo and Tsai, Rev. Mod. Phys., 41 (1969) 205.
- <sup>2</sup>J. W. Chapman, et al., Phys. Rev. D14 (1976) 5.
- <sup>3</sup>Goldhaber, et al., Phys. Rev. Lett. 37 (1976) 255; I. Peruzzi, et al., Phys. Rev. Lett. 37 (1976) 569.
- <sup>4</sup>E. G. Cazzolie, et al., Phys. Rev. Lett. 34 (1975) 1125.
- <sup>5</sup>J. P. Berge, et al., Fermilab preprint, November 1975 (unpublished).
- <sup>6</sup>S. J. Barish, et al., Phys. Lett. 66B (1977) 291.

## APPENDIX A

### Details of the ITC

(1) Construction: Each plate will be 0.9 cm thick and have radius 3-6" less than the chamber section at the corresponding place to allow for liquid circulation. The top of each plate will terminate at the plane given by  $Z = 70$  cm. If deemed advisable, a 4" x 18" rectangular hole will be cut in the center of each plate for a hadron beam window for possible ITC hadron experiments. Also a small (approximately 6" x 24") rectangular slot will be cut at the bottom of plates #2, #3, #7 and #8 as a manway for additional welding between in-place plates. These two sets of openings will reduce the area and mass of the plates by less than 1%. Since the piston part will not allow a plate with minimum dimension more than 6 ft. to pass through, plates #2-8 will each be installed in two half sections which may either be joined or else separated by a few centimeters. To allow visibility in View #1, the upstream surface of each plate will be chrome plated and possibly overcoated with silicon dioxide. Scotchlite strips will be put on the uppermost edge of each plate to render them almost invisible in Views #5 and 6. This will facilitate scanning and will allow plate numbers and additional fiducial crosses to be inked on. Each plate section will be mounted on brackets which have been pre-welded on the chamber wall.

(2) Boiling Considerations: Many experiments with plates show that negligible boiling occurs around the plates as long as edges are smooth, small crevices are absent and conditions resulting in high local velocities of the liquid are eliminated.

For example, the BNL 7 ft. chamber has run successfully with four large area plates closely spaced and has exhibited almost no boiling.

(3) Mechanical Strength: If stress analyses show that excessive flexing of the plates occurs during expansion, three different solutions exist. (i) use a lower Z material such as Ti, which would then require 1.8 cm thick plates, (ii) weld 1" diam. stainless steel rods as a bridge from plate to plate, (iii) suspend the plates on heavy springs at each bracket so the plates will move an inch with the liquid.

## APPENDIX B

Comparison of ITC, Downstream Plates (DP), TST and H-Ne.

Parameter	ITC	DP	TST	H-Ne (atomic)	
				20%	100%
Ave. $\gamma$ detection efficiency	90%	90%	90%	70%	99%
$\delta P/P$ for $\pi^0$ (before fitting)	17%	>20%	8%	6%	10%
H <sub>2</sub> fiducial volume (m <sup>3</sup> )	16	~10	~	-	-
Heavy nucleus fiducial mass (tons)	4.5	-	~15	5.2	26
Ability to measure $\sigma(n)/\sigma(p)$	exc.	poor	good	poor	poor
Ability to study $V^0$ decays	exc.	exc.	exc.	exc.	good
Ability to study kink decays	exc.	exc.	exc.	poor	poor
$\mu$ detection efficiency (>2 GeV)	>95%	>95%	>95%	>95%	>95%
e detection efficiency (after measurement)	>95%	>90%	>95%	>95%	>97%

TABLE I  
 YIELDS OF NEUTRINO EVENTS INSIDE  
 FIDUCIAL VOLUME FOR ITC  
 (based on E45 measurements)

Reaction	Number of Events <sup>*</sup>
$\nu p \rightarrow \mu^- X$	12,000
$\nu p \rightarrow \nu X$	3,000 <sup>†</sup>
$\nu p \rightarrow \Lambda X$	600 <sup>‡</sup>
$\nu p \rightarrow K_s^0 X$	600 <sup>‡</sup>
$\nu p \rightarrow \mu^- e^+ X$	120
$\nu p \rightarrow \mu^- \mu^+ X$	120
TOTAL $\nu p$	15,000
$\nu \text{Nuc} \rightarrow \mu^- X$	73,000
$\nu \text{Nuc} \rightarrow \nu X$	12,000
$\nu \text{Nuc} \rightarrow \mu^- e^+ X$	730
$\nu \text{Nuc} \rightarrow \mu^- \mu^+ X$	730
TOTAL $\nu \text{Nuc}$	85,000
$\nu_\mu e^- \rightarrow \mu^- \nu_e$	~40 (~120 <sup>#</sup> )
$\nu_\mu e^- \rightarrow \nu_\mu e^-$	~50 (~150 <sup>#</sup> )
TOTAL $\nu_\mu e$	90 (270 <sup>#</sup> )
TOTAL NEUTRINO EVENTS	100,000

<sup>\*</sup> 300K pictures,  $1.3 \times 10^{13}$  ppp, 400 GeV/c protons, 2 horns, 16 m<sup>3</sup> fid. vol.,  $\Sigma P_x$  (vis.) > 9 GeV/c.

<sup>†</sup>  $\Sigma P_x$  (vis.) > 5 GeV/c for neutral current events.

<sup>‡</sup> charged (i.e., visible) decays only.

<sup>#</sup> including events from plates.

TABLE II  
 RESOLUTION FOR BARE H<sub>2</sub> CHAMBER AND FOR ITC  
 WITH H<sub>2</sub>

Variable	Charged current events		Neutral current events	
	Bare H <sub>2</sub>	ITC + H <sub>2</sub>	Bare H <sub>2</sub>	ITC + H <sub>2</sub> <sup>*</sup>
E <sub>v</sub>	~8%	~2%	unmeasurable	~20%
x	~.03	~.007	"	~0.1
y	~.04	~.01	"	~0.1
q <sup>2</sup>	~8%	~2%	"	~20%
v	~16%	~4%	"	~ 5%
W	~8%	~2%	"	~ 7%

Note: Numbers quoted as percentages are fractional resolutions and decimal numbers are absolute resolutions

\* For final states with measurable baryons such as p,  $\Lambda$ ,  $\Sigma$ , np + pp $\pi^-$ , etc.

$\gamma$  CONVERSION PROB.

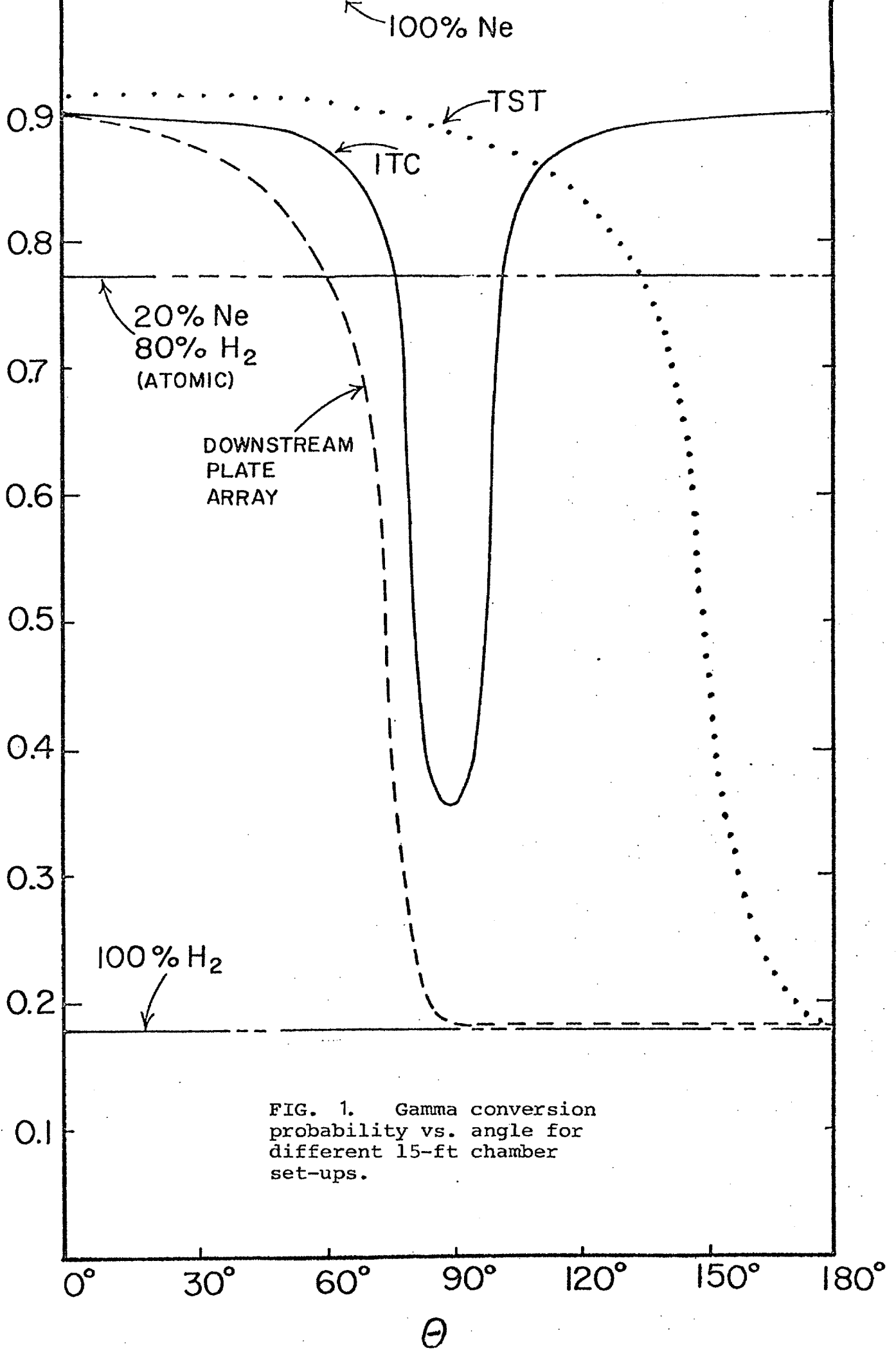
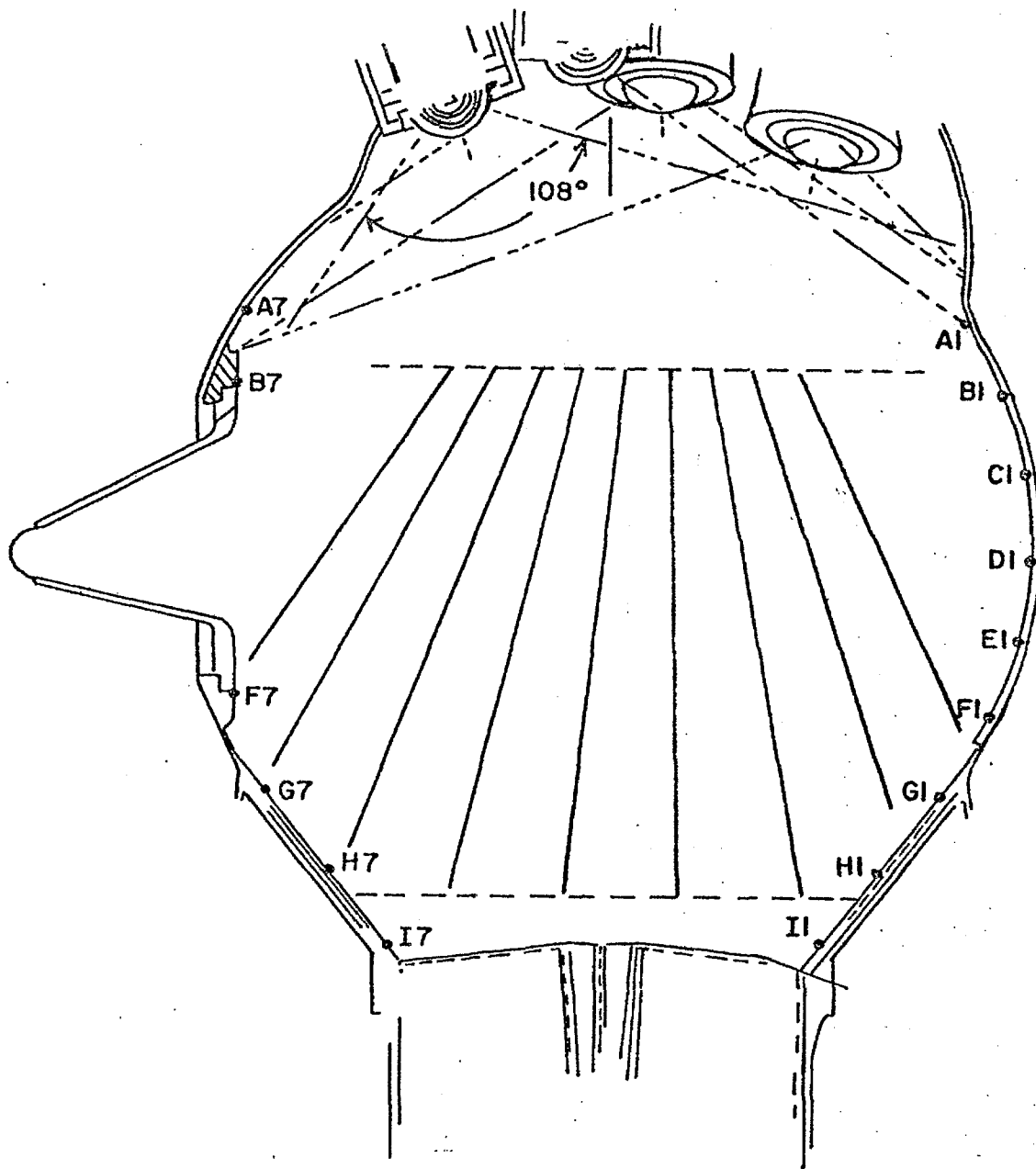
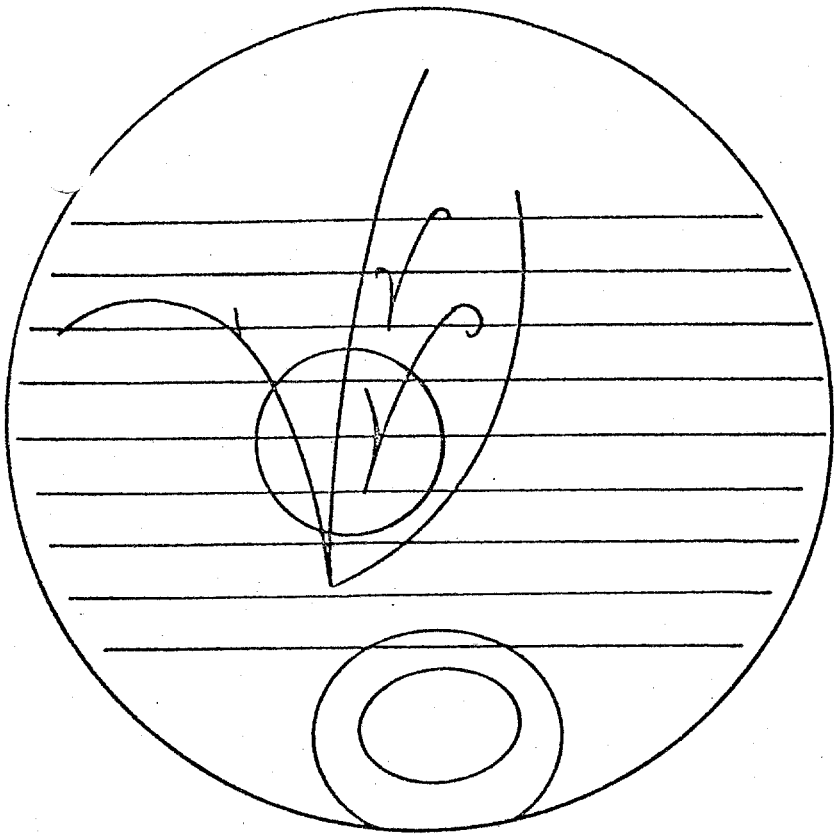


FIG. 1. Gamma conversion probability vs. angle for different 15-ft chamber set-ups.



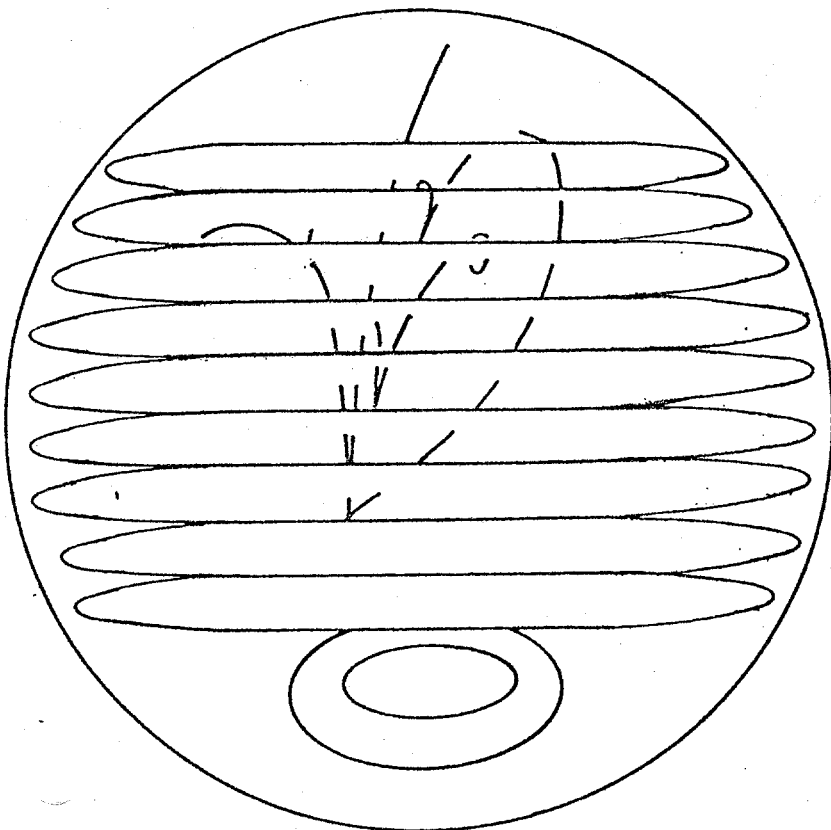
15-F.T. CHAMBER WITH ITC  
(side view)

FIG. 2(a)

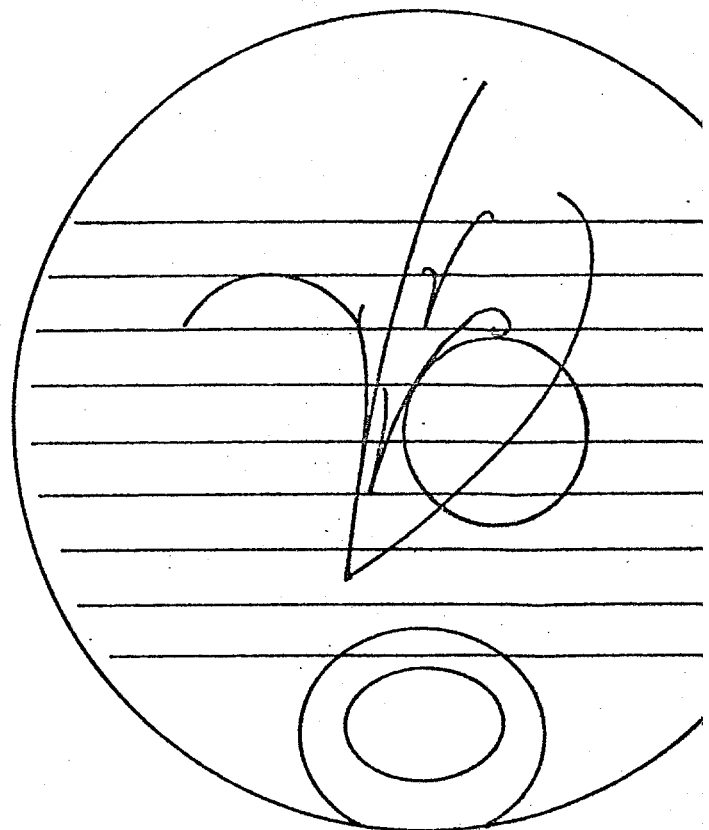


VIEW 5

3-PRONG +  $\pi^0$



VIEW 1



VIEW 6

FIG. 2 (b)

$$\phi(\alpha, t)$$

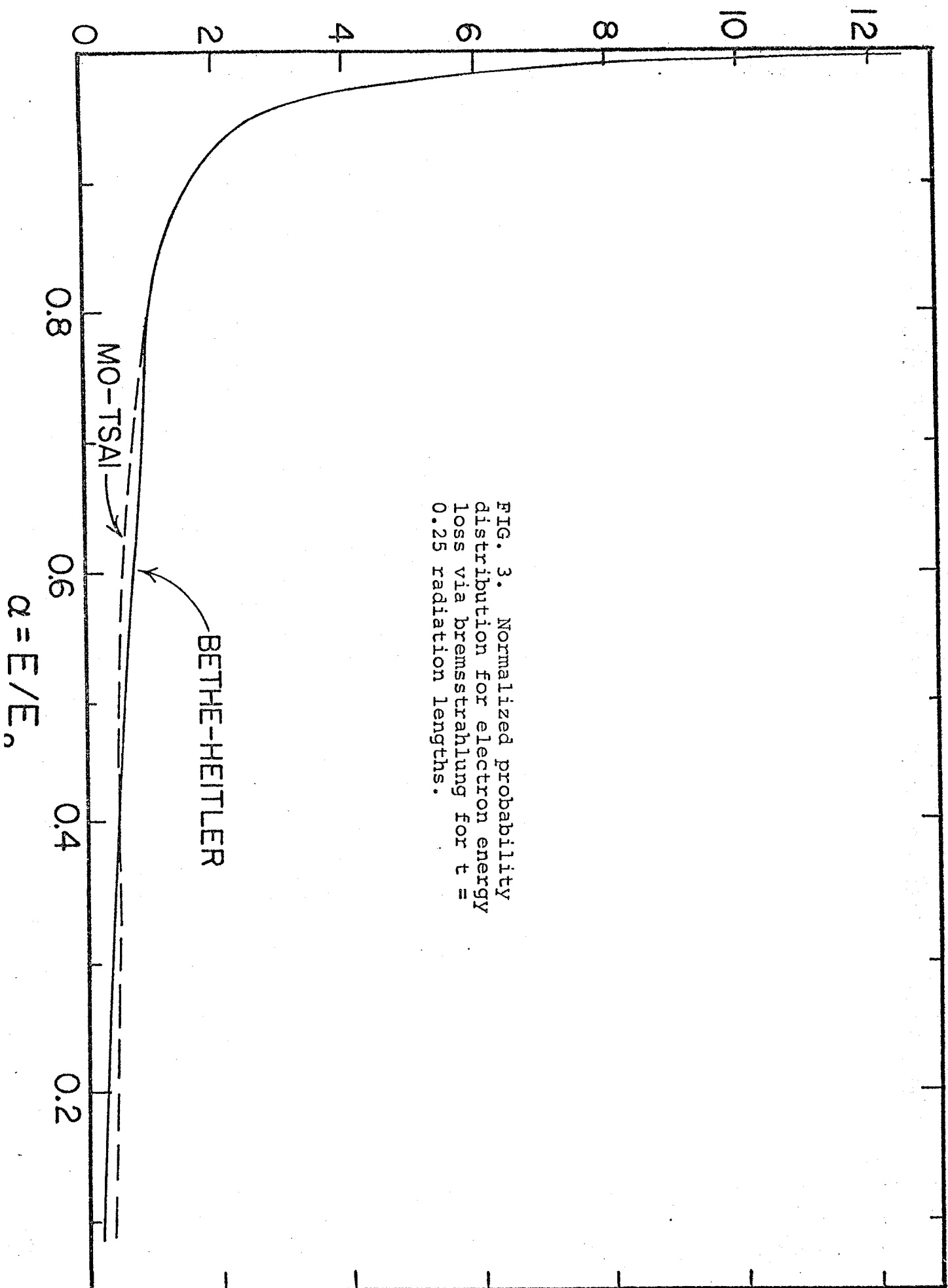


FIG. 3. Normalized probability distribution for electron energy loss via bremsstrahlung for  $t = 0.25$  radiation lengths.